environmental microbiology
environmental microbiology reports

Influence of the Hfq and Crc global regulators on the control of iron homeostasis in Pseudomonas putida

Journal:	*Environmental Microbiology and Environmental Microbiology Reports*
Manuscript ID	EMI-2018-0630.R1
Journal:	Environmental Microbiology
Manuscript Type:	EMI - Research article
Date Submitted by the Author:	n/a
Complete List of Authors:	Sánchez-Hevia, Dione; Centro Nacional de Biotecnología, CSIC, Biotecnología Microbiana Yuste, Luis; Centro Nacional de Biotecnología, CSIC, Biotecnología Microbiana Moreno, Renata; Centro Nacional de Biotecnología, CSIC, Biotecnología Microbiana Rojo, Fernando; Centro Nacional de Biotecnología, CSIC, Biotecnología Microbiana;
Keywords:	bacteria, gene expression/regulation, genomics/functional genomics/comparative genomics, metabolic networks, metals

+

Influence of the Hfq and Crc global regulators on the control of iron homeostasis in *Pseudomonas putida*

Dione L. Sánchez-Hevia, Luis Yuste, Renata Moreno* and Fernando Rojo*

Departamento de Biotecnología Microbiana, Centro Nacional de Biotecnología, CSIC, Darwin 3, Cantoblanco, 28049 Madrid, Spain

***E-mail of Corresponding authors**: frojo@cnb.csic.es; rmoreno@cnb.csic.es

E-mail of co-authors: dlsanchez@ cnb.csic.es; lyuste@cnb.csic.es

Tel: (+34) 91 585 45 39; **Fax**: (+34) 91 585 45 06

Running title: Hfq and Crc influence on iron homeostasis

Key words: Translational regulation, Global regulation, Catabolite repression, Carbon metabolism, iron metabolism, RNA binding

SUMMARY

Metabolically versatile bacteria use catabolite repression control to select their preferred carbon sources, thus optimizing carbon metabolism. In pseudomonads, this occurs through the combined action of the proteins Hfq and Crc, which form stable tripartite complexes at target mRNAs, inhibiting their translation. The activity of Hfq/Crc is antagonised by small RNAs of the CrcZ family, the amounts of which vary according to carbon availability. The present work examines the role of *Pseudomonas putida* Hfq protein under conditions of low-level catabolite repression, in which Crc protein would have a minor role since it is sequestered by CrcZ/CrcY. The results suggest that, under these conditions, Hfq remains operative and plays an important role in iron homeostasis. In this scenario, Crc appears to participate indirectly by helping CrcZ/CrcY to control the amount of free Hfq in the cell. Iron homeostasis in pseudomonads relies on regulatory elements such as the Fur protein, the PrrF1-F2 sRNAs, and several extracytoplasmic sigma factors. Our results show that the absence of Hfq is paralleled by a reduction in PrrF1-F2 small RNAs. Hfq thus provides a regulatory link between iron and carbon metabolism, coordinating the iron supply to meet the needs of the enzymes operational under particular nutritional regimes.

Originality-Significance Statement

The Hfq protein is a riboregulator present in many bacterial groups; it controls mRNA translation by facilitating the annealing between small RNAs and their target mRNAs, or by forming complexes at the translation initiation regions of mRNAs. It can influence the stability of many small RNAs. In pseudomonads, Hfq, together with the regulatory protein Crc, helps to optimize carbon metabolism via the so-called catabolite repression response. Hfq and Crc form tripartite ribonucleoprotein complexes at specific target sites, inhibiting the initiation of translation of affected mRNAs. The activity of Crc/Hfq is antagonised by small RNAs of the CrcZ family, the amounts of which vary strongly according to carbon availability. In *Pseudomonas aeruginosa*, Hfq also influences virulence and quorum sensing. The present work examines the role of *Pseudomonas putida* Hfq protein under conditions of low-level catabolite repression control, under which Crc protein is believed to play a minor role. The results support the idea that, under conditions in which most Crc molecules are sequestered by CrcZ and CrcY, Hfq still performs important regulatory functions, implying that a significant amount of free Hfq must remain. Indeed, the present work shows that Hfq participates in the orchestration of iron homeostasis, at least in part by controlling the levels of PrrF1 and PrrF2 sRNAs. Crc appears to have an indirect role in controlling the amount of free Hfq, perhaps by facilitating the formation of stable Crc-Hfq-CrcZ/CrcY complexes.

Introduction

Pseudomonas putida, a Gram-negative bacterium, can colonize different environments such as soils, the rhizosphere, and aquatic systems (Wu et al., 2011; Udaondo et al., 2016). This is in part due to its capacity to endure many kinds of stress (Martínez-García and de Lorenzo, 2011; Moreno and Rojo, 2014; Ramos et al., 2015), but also to its ability to exploit a wide range of carbon sources (Nelson et al., 2002; Belda et al., 2016). These properties, and its non-pathogenic status that allowed its certification as a safety strain by the Recombinant DNA Advisory Committee (Fedral-Register, 1982), render *P. putida* an interesting model organism of great potential in industrial biotechnology (Poblete-Castro et al., 2012; Nikel et al., 2014). Key to its metabolic versatility is its efficient control of the uptake and metabolism of nutrients, allowing cells to assimilate many of them in a hierarchical and sequential order; its metabolism is adjusted to each situation, optimizing energy gains (Shingler, 2003; Rojo, 2010). The global regulatory system instrumental in organizing the most appropriate metabolic configuration relies on the combined action of the proteins Hfq and Crc, the CrcZ and CrcY small RNAs (sRNAs), and the CbrA/CbrB two-component system.

Hfq is an abundant RNA-binding protein present in most bacterial species; it recognizes specific targets in RNAs and has a key role in post-transcriptional gene regulation. In *Escherichia coli*, and probably many other bacterial species, Hfq facilitates the annealing of sRNAs to their target mRNAs, ultimately modulating their translation and stability (for reviews see Vogel and Luisi, 2011; Wagner and Romby, 2015; Updegrove et al., 2016). In pseudomonads, the inactivation of the *hfq* gene results in a general reduction in physiological performance. In *P. putida*, a lack of Hfq has consequences on cell morphology, growth on a number of carbon sources, cell motility, and the regulation of the stress-related σ^S sigma factor. In addition, Hfq-deficient cells have lower ATP and NADPH contents and are more sensitive to oxidative stress and UV light (Arce-Rodríguez et al., 2016). Inactivation of the *hfq* gene in *P. aeruginosa* also results in pleiotropic effects that

influence cell motility and growth under anoxic conditions, as well as causing redox imbalances, altered quorum-sensing responses, and significantly attenuated virulence (Sonnleitner et al., 2003; Sonnleitner et al., 2006; Pusic et al., 2016). In pseudomonads, Hfq assists the annealing of regulatory sRNAs to their target mRNAs (Ferrara et al., 2015), but part of its regulatory function is performed in cooperation with the Crc (catabolite repression control) protein, which has been found only in this bacterial group and certain related genera (reviewed in Rojo, 2010; see also Quiroz-Rocha et al., 2017). Crc is a global regulator that modulates the expression of many genes, helping to control carbon metabolism. It acts post-transcriptionally, inhibiting the translation of mRNAs containing an AAnAAnAA motif close to the ribosome binding site. This motif is initially recognized by Hfq, the role of Crc being to stabilize Hfq-binding as a tripartite Hfq-RNA-Crc complex (Moreno et al., 2009b; Sonnleitner et al., 2009; Madhushani et al., 2015; Moreno et al., 2015; Sonnleitner et al., 2017).

The activity of Hfq and Crc is antagonized by the CrcZ and CrcY sRNAs. These sRNAs are very similar to one another in sequence and contain several A-rich Hfq target motifs that bind and sequester Hfq and Crc to form a Crc-Hfq-CrcZ/Y complex (Sonnleitner et al., 2009; Moreno et al., 2012; Sonnleitner and Blasi, 2014; Madhushani et al., 2015; Moreno et al., 2015; Hernández-Arranz et al., 2016). The levels of these two sRNAs vary greatly depending on growth and/or physiological conditions, being lower when cells use rich carbon sources that allow for rapid growth, and much higher when non-preferred carbon sources are used (Valentini et al., 2014, and references cited above). This presumably allows Hfq/Crc activity to be adapted to cell needs, with metabolism adjusted accordingly. The amount of CrcZ and CrcY in the cell depends on an equilibrium between their transcription from promoters *PcrcZ* and *PcrcY* respectively, and their degradation. These promoters are recognized by a form of RNA polymerase bound to the RpoN sigma factor and require the CbrB transcriptional activator. CbrB is phosphorylated by CbrA sensor kinase in response to a still unknown signal (Sonnleitner et al., 2009; Moreno et al.,

2012; García-Mauriño et al., 2013). The binding of Hfq and Crc to CrcZ and CrcY protects them from degradation by RNases (Hernández-Arranz et al., 2016).

The inactivation of the *crc* gene in *P. putida* and *P. aeruginosa* results in phenotypes characterized by an unbalanced metabolism, an altered hierarchy of the uptake and assimilation of carbon sources, increased antibiotic susceptibility, and reduced fitness (MacGregor et al., 1992; Moreno et al., 2009a; Linares et al., 2010; Hernández-Arranz et al., 2013; La Rosa et al., 2014; La Rosa et al., 2015). These phenotypes have also been observed for an Hfq-null strain, although *hfq* inactivation has a much more severe effect than the inactivation of *crc*. Since many of the Hfq-dependent phenotypes are not seen in Crc-null strains, but Crc needs Hfq to exert its functioning, it would seem that Hfq can regulate some genes on its own but needs Crc to control a specific subset of genes.

The aim of the present work was to identify the genes regulated by Hfq but not by Crc, and to determine the possible function of Hfq and Crc when cells grow using just one carbon source. This was undertaken by comparing the transcriptome and proteome of Crc-null, Hfq-null and Crc/Hfq-null strains to those of the wild type strain. Cells were cultured in a mineral salts medium containing succinate as the carbon source. This was used for several reasons. First, the growth rate of the Crc-null and the Hfq-null strains in this medium is similar to that of the wild type strain (see Fig. S1, supplementary material), which facilitates comparison. And second, when *P. putida* grows at the expense of succinate as the sole carbon source, the levels of CrcZ and CrcY are relatively high, and a large proportion of the Hfq/Crc molecules would therefore be sequestered by these sRNAs (La Rosa et al., 2015). *Pseudomonas putida* shows only a moderate preference for succinate as a carbon source, which agrees with Crc being mostly non-functional when cells use this substrate (Yuste et al., 1998; Hester et al., 2000; Daniels et al., 2010; La Rosa et al., 2015; reviewed in Rojo, 2010). However, Hfq ought to remain present at sufficient levels to perform its Crc-independent regulatory functions. The results presented here show that, when cells use succinate as the sole carbon source, Hfq still regulates genes that are, for the most part, unrelated to carbon catabolism. Indeed, Hfq was found to

have an important role in controlling iron metabolism. This supports the idea that the CrcZ/Y present in cells growing on succinate sequester most of the Crc molecules available, but enough Hfq remains to control other genes through mechanisms that rely on other sRNAs, such as those involved in iron homeostasis.

Results and Discussion

Inactivation of the crc *or* hfq *genes modifies the expression of a significant number of genes under the conditions analysed: general view*

Earlier work has shown that, although Crc and Hfq are post-transcriptional regulators, their absence has an important influence on the transcriptome since they inhibit the translation of mRNAs for several transcriptional regulators as well as for proteins involved in the uptake of substrates which in turn induce the expression of catabolic pathways, inhibition that can also reduce mRNA stability (Sonnleitner et al., 2006; Moreno et al., 2009a; Hernández-Arranz et al., 2013; Grenga et al., 2017). To gain initial insight into the influence of Hfq and Crc in cells growing in a minimal salts medium containing succinate as the sole carbon source, the transcriptomic profile of wild-type *P. putida* KT2440 was compared to that of its *hfq*, *crc* and *hfq crc* mutant derivatives. Since earlier work had shown that the effect of Crc/Hfq is particularly manifest during the exponential phase of growth (Moreno et al., 2012), total RNA was obtained from exponentially growing cells (A_{600}=0.6) and the transcriptomes analysed by directional RNA-seq deep sequencing. RNAs levels more than 3-fold ($\log_2$ of 1.58) different between the strains compared, and for which the false discovery rate (FDR) was ≤0.01, were considered differentially expressed. With these cut-off values, the inactivation of *crc* led to changes in the mRNA abundance of 82 genes, while the lack of *hfq* affected 179 genes (Supplementary Tables S1 and S2). The inactivation of both *crc* and *hfq* modified the mRNA levels of 301 genes (Table S3).

When comparing the transcriptomes of the mutant strains to that of the wild type, most of the differentially expressed genes corresponded to either hypothetical proteins or proteins with an unknown function, or to those involved in the binding and transport of substrates, regulatory functions, or energy metabolism (Fig. S2). In the Crc-null strain, most of the genes affected had lower mRNA levels than the wild type strain; this was less pronounced in the Hfq-null strain.

Unexpectedly, the transcriptome of the Hfq-null strain showed no RNA reads for the region spanning genes PP_3849 to PP_3920, except for gene PP_3868. This region corresponds to prophage 1, one of the four prophages identified in this bacterial strain (Wu et al., 2011; Martínez-García et al., 2015b). PCR amplification using primers specific for the genes located at one of the ends of the non-expressed phage genes (direct primer hybridizing at PP_3849, and inverse primer at PP_3850) rendered a clear amplification signal when using chromosomal DNA from the wild type strain, but not when using DNA from the Hfq-null strain (Fig. S3). A similar result was obtained when using a primer pair directed towards the genes of the other end of prophage 1 (genes PP_3919 and PP_3920). This shows that prophage 1 is not present in the Hfq-null strain. The reads assigned to gene PP_3868, which is located in the central region of the prophage and codes for a protein with similarity to group II intron-encoding maturases, likely correspond to any of the seven other genes present in the KT2440 genome that show >97% nucleotide similarity to PP_3868; these reads were most likely incorrectly assigned to PP_3868 by the software used. In summary, prophage 1 was concluded absent in the Hfq-null strain.

Although the RNA levels of some genes corresponding to prophages 2 and 3 were higher in the Hfq-null strain than in the wild type, the changes observed did not pass the filters set to consider a gene as differentially expressed. However, 11 of the 52 genes conforming prophage 4 (PP_1532 to PP_1584) were clearly overexpressed in the Hfq-null strain (Table S2). The altered expression of prophage 4 in the Hfq-null strain, as well as the absence of prophage 1, suggest that Hfq might affect the regulation of the

lysis/lysogeny decision, either directly or as a consequence of the metabolic stress known to occur in this mutant strain (Martínez-García et al., 2015b).

Since Hfq and Crc are post-transcriptional regulators, the effect of their absence on the proteome was also analysed in cells cultured under the same conditions used in the RNA-seq assays. Proteins were analysed using the iTRAQ procedure (see Experimental Procedures); only those proteins identified with FDR≤ 0.01 were taken into consideration. The relative levels of 1418 proteins for the Crc-null strain, of 1419 for the Hfq-null strain, and of 1410 for the *crc hfq* double mutant, were compared to those of the wild type strain. Proteins with a ≥1.4 fold (log_2 of 0.49) change in abundance, and with a *q*-value of ≤0.05, were considered differentially expressed. The expression of 10 proteins was altered in the *crc* mutant compared to the wild-type strain (Table S4). In the *hfq* mutant, the levels of 54 proteins were affected (Table S5). In the double mutant, 81 proteins were differentially expressed (Table S6). Fifteen of the differentially expressed proteins correspond to mRNAs containing a putative A-rich Hfq binding site at their 5' end (Table S7). This included proteins involved in the uptake and assimilation of amino acids (HmgA, AatJ or BkdA1) or sugars (Gap-1), the expression of which is known to be regulated by Hfq/Crc (Hester et al., 2000; Morales et al., 2004; Moreno et al., 2009a). Interestingly, many proteins differentially expressed in the iTRAQ assays showed no detectable changes in the RNA-seq assays, which is suggestive of post-transcriptional regulation (for 9 genes in the *crc* mutant strain, 46 in the *hfq* mutant strain, and 61 in the double mutant; Table S7).

Effect of inactivating the crc *gene on the transcriptome and proteome of the cell*

Both the transcriptomic and proteomic assays indicated that, in the minimal medium with succinate used to culture the cells, the absence of Crc had a significantly smaller influence than that observed in earlier reports in which cells had been cultured in LB complete medium (Moreno et al., 2009a). This is consistent with the observation that the amount of CrcZ+CrcY present in cells growing exponentially in M9 medium with succinate

is more than 7 fold that seen in cells cultured in LB medium (La Rosa et al., 2015). This suggests that when cells grow in M9 succinate medium there is less Crc and/or Hfq available to control gene expression than in LB medium. In addition, a large proportion of the genes actively regulated by Crc/Hfq in cells cultured in LB were not induced in the succinate medium, or expressed at very low levels, as might be expected for a metabolism in which succinate is the sole carbon source.

It is worth noting, however, that many of the genes for which expression changed when Crc was lacking appeared not to be influenced by the absence of Hfq. Only 30 out of the 179 genes regulated by Hfq also showed a change in the Crc-null strain (Fig. 1). At first glance this is surprising since, if Crc strictly needs Hfq to exert its regulatory function (as is believed), it might be argued that all genes that are differentially expressed by the absence of Crc should also show altered expression in the Hfq-null strain. However, it should be taken into account that when cells grow in the M9 succinate medium used a large part of the Hfq and Crc molecules are trapped by CrcZ/CrcY and, if Crc is absent, the complexes formed by Hfq with these two sRNAs would be unstable (Moreno et al., 2015; Sonnleitner et al., 2017). In addition, inactivation of the *crc* gene leads to a strong decrease in CrcZ and CrcY levels (García-Mauriño et al., 2013; Hernández-Arranz et al., 2016). Thus, the Crc-null strain would have significantly larger amounts of free Hfq protein than the wild type strain. Since Hfq can regulate genes in a Crc-independent manner, for example by facilitating the annealing of sRNAs to target mRNAs, the larger amounts of free Hfq present in the Crc-null strain might impact the expression of several genes that would otherwise not be regulated by Hfq in the wild type strain. An alternative explanation for the existence of genes deregulated in the Crc-null strain, but not in the Hfq-null strain, is that Crc might also exert a regulatory function with the aid of a protein other than Hfq. Although there is currently no direct evidence for this, it would help explain the unexpected observation that the number of differentially expressed genes in the double mutant (301 genes in the RNA-seq assays) was greater than that seen in the Hfq-null strain (179

genes). If Crc strictly needs Hfq for RNA binding, the number of genes affected in the Hfq-null strain ought to be similar to that of the double mutant.

The changes in RNA levels detected in the Crc-null strain were, in most cases, small, and the affected genes generally not grouped into operons (Table S1). The possible differential expression of 16 of these genes was also analysed by real-time RT-PCR, which in only 10 cases revealed a change of greater than 2-fold (Table S8). The proteomic assays detected changes in only 10 proteins, half of them ribosomal. This agrees with Crc playing a minor role under the conditions tested. It is worth noting, however, that the RNA levels for 16 pyoverdine-related genes showed a clear reduction in the Crc-null strain (Fig. 2B). This was confirmed by real-time RT-PCR in the three cases tested, although the fold-change values recorded were lower than those seen in the RNA-seq assays (Table S8). Since the expression of all these genes was also affected by the absence of Hfq, these results are discussed below with those for the latter protein.

Among the genes for which RNA levels increased in the absence of Crc were those for the high affinity transport system for succinate and fumarate, *dctPQM*. The expression of these genes is known to be repressed post-transcriptionally by Crc in both *P. putida* (La Rosa et al., 2015) and *P. aeruginosa* (Valentini and Lapouge, 2013). In fact, both *P. putida* *dctP* and *dctM* contain Hfq/Crc binding sites at their translation initiation regions. Inhibition of *dctPQM* mRNA translation by Crc/Hfq is paralleled by a reduction in the abundance of this RNA, probably because it is degraded more efficiently (La Rosa et al., 2015). With the filters used here, only *dctM* appeared to be regulated by Crc (RNA levels were three times those recorded for the Crc-null strain; $P<0.008$), although less restrictive filtering showed *dctP* and *dctQ* mRNA levels to be somewhat higher in the Crc-null strain (1.9-fold, for *dctP*, and 1.8-fold, for *dctQ*). The DctPQM transport system plays a major role at micromolar concentrations of succinate, although at the millimolar concentrations used here, succinate uptake also occurs through the DctA transporter, the expression of which is not repressed but rather stimulated indirectly by Crc in *P. aeruginosa* (Valentini and

Lapouge, 2013). In *P. putida*, the expression of *dctA* appears to be independent of Crc (La Rosa et al., 2015; this work).

Effect of inactivating the hfq *gene on the transcriptome and proteome: iron homeostasis*

Of the 179 genes for which mRNA levels were altered in the Hfq-null strain, 77 corresponded to prophages, hypothetical proteins, or genes of unknown function. Among the remaining 102 genes, 41 were related to iron metabolism, 21 were involved in the transport and metabolism of amino acids, acetoin or other compounds, 13 corresponded to different components of the electron transport chain, 6 were related to cellular stress, while the rest were associated to diverse functions.

Expression of the genes corresponding to the terminal oxidases Cbb3-1 and Aa3 of the electron transport chain all showed reduced expression in the Hfq-null strain. *Pseudomonas putida* has a branched electron transport chain with multiple terminal oxidases, the relative proportion of which vary according to environmental and physiological conditions (Ugidos et al., 2008; Sevilla et al., 2013). The altered expression of Cbb3-1 and Aa3 terminal oxidases is therefore likely related to an adjustment in the configuration of the electron transport chain to meet the energy demands of the mutant strain. In the light of the general effects on the cell caused by the lack of Hfq, some adjustments in metabolism might be expected. This would explain the altered expression of the genes corresponding to porins and the catabolism of acetoin and amino acids. However, the large number of genes involved in iron homeostasis that showed an altered expression in the strain lacking Hfq indicates that this protein plays an important role in iron metabolism. This was analysed in further detail.

Iron acts as an essential cofactor for many enzymes involved in carbon assimilation and energy metabolism. Although abundant in soils, under aerobic conditions iron is primarily present in its oxidized form, Fe(III), which is very insoluble in water. Pseudomonads have complex iron uptake systems and secrete siderophores with high-

affinity for Fe(III) (reviewed in Cornelis, 2010; Schalk and Guillon, 2013; Schalk and Cunrath, 2016). Once Fe(III) has formed a complex with either a heme or an iron-siderophore (such as pyoverdine), it binds to a specific outer membrane receptor with a gate on its periplasmic side. This gate opens upon interaction with the TonB protein which, together with the ExbB and ExbD proteins, transmits the energy needed to open the gate. The ferrisiderophore thus gains access to the periplasm and, with the help of a periplasmic binding protein, is taken by a transporter to the cytoplasm. Here, Fe(III) is reduced to Fe(II) and incorporated into iron-containing proteins. The siderophore is either degraded or recycled.

Although essential for life, iron can be toxic if present in excessive amounts. Thus, the expression of the genes involved in iron uptake is regulated according to the cytoplasmic concentration of Fe(II). This primarily involves the Fur repressor, a number of sigma and anti-sigma factors, and two small RNAs (PrrF1 and PrrF2). The mechanisms entailed have been mostly studied in *P. aeruginosa*, but the key features (though perhaps not the details) are likely conserved in *P. putida* (reviewed in Cornelis et al., 2009; Schalk and Guillon, 2013; Llamas et al., 2014; Schalk and Cunrath, 2016). When the intracellular concentration of Fe(II) is sufficiently high, it binds to the Fur protein, and the Fur-Fe(II) complex binds to DNA at sites containing the so-called Fur boxes. This represses the transcription of several genes involved in iron acquisition, such as those coding for the iron-starvation extra-cytoplasmic function (ECF) sigma factors and the TonB-dependent transporters of ferrisiderophores. The consequence is a reduction of iron uptake, limiting its toxicity. The iron-starvation ECF sigma factors are required to direct the RNA polymerase to specific genes involved in iron uptake and homeostasis. Under iron limitation conditions, iron-starvation ECF sigma factors are expressed but their activity is inhibited by a cognate anti-sigma factor. Activation of iron starvation ECF sigma factors usually occurs in response to a specific iron-scavenging molecule and involves a signal transduction cascade known as cell-surface signalling (CSS) that, besides the iron starvation ECF and the anti-sigma factors, also involves an outer membrane TonB-

dependent receptor. CSS receptors have a dual function in signalling and in transport of the iron-scavenging molecule (Llamas et al., 2014).

Fur-Fe(II) also represses the transcription of the genes specifying the PrrF1 and PrrF2 sRNAs, which in turn inhibit the expression of several genes coding for proteins that contain iron, such as succinate dehydrogenase (*sdh*) and superoxide dismutase (*sodB*) (Wilderman et al., 2004). Thus, under iron-sufficient conditions, Fur indirectly activates the expression of iron-containing proteins. When iron becomes limiting, Fur detaches from DNA and repression is relieved, allowing the production of iron scavenging molecules such as pyoverdine, the iron-starvation ECF sigma factors, and PrrF1 and PrrF2 sRNAs (reviewed in Cornelis et al., 2011). These sRNAs reduce the production of iron-containing proteins, helping to modify the enzyme load of the cell towards a configuration requiring less iron. The secretion of pyoverdine allows for Fe(III) scavenging. In addition, upon transport of the ferripyoverdine complex through the outer membrane receptor, a signal is transduced to the periplasmic domain of an anti-sigma factor that is transmitted to its cytoplasmic domain. This causes the release of the sequestered ECF sigma that can then bind the RNA polymerase core and direct it to transcribe the iron-starvation genes. *Pseudomonas putida* KT2440 contains 13 ECF sigma factors presumably involved in iron acquisition, all of which are associated genomically and/or functionally with anti-sigma factors (Martínez-Bueno et al., 2002; Llamas et al., 2014). Eleven of these anti-sigma factors map adjacent to the sigma factor. For the other two, PvdS (ECF4) and FpvI (ECF6), the association is only functional. Although not experimentally analyzed yet, by analogy with *P. aeruginosa* these two sigma factors are likely involved in KT2440 pyoverdine production and uptake, respectively, and their activity is likely controlled by the anti-sigma factor FpvR (PP_3555) and by the TonB-dependent receptor FpvA (PP_4245) (Llamas et al., 2014). For 12 of the above sigma factors, the sigma/anti-sigma gene cluster also includes a gene coding for a ferric siderophore receptor or a heme receptor.

P. putida KT2440 produces pyoverdine, a high affinity siderophore; there is no experimental evidence to suggest it produces any other (Matthijs et al., 2009). The

inactivation of *hfq* led to a reduction in the mRNA levels of several genes believed involved in the synthesis and export of pyoverdine. Reductions were also seen for those representing the gene cluster PP_3798 to PP_3804, which codes for a cation ABC transporter and other membrane proteins (Fig. 2 and Table S2). Expression of the genes for the iron-storage protein bacterioferritin were reduced as well. Real-time RT-PCR analysis for some of these genes confirmed this reduction (see Table S8) and showed that the mRNA levels of some neighbour genes that did not show up in the RNA-seq assays either decreased (PP_3797, *fpvA*, PP_4245) or increased (*pvdS*). Although the proteomic analyses did not detect the proteins corresponding to most of the genes listed in Fig. 2, they showed that proteins PvdA, FpvA, PvdH and PvdL were downregulated when Hfq was lacking (Tables S5 and S6), which is in line with the results observed in the RNA-seq assays. In contrast, the Hfq-deficient strain showed increased expression of several genes involved in the uptake of siderophores, such as those for several TonB-dependent ferric siderophore receptors, seven iron-related ECF sigma factors and their adjacent anti-sigmas, and the *exbB-exbD-tonB* genes that code for the TonB energy transducing system, which provides the energy required for the uptake of siderophores (Tables S2, S3 and S8; Fig. 2). The substrate specificity of several of these siderophore receptors has been determined or proposed by analogy to those of *P. aeruginosa*. FpvA transports pyoverdine, while other receptors interact with siderophores produced by other microorganisms (e.g. aerobactin, ferrioxamine, ferrichrome; Cornelis and Matthijs, 2002; Schalk, 2008; Llamas et al., 2014). For example, IutA (PP_2193) is an aerobactin receptor (Bastiaansen et al., 2014) while FoxA (PP_0160) interacts with ferrioxamine (Llamas et al., 2006; Bastiaansen et al., 2015). Proteomic assays also showed FoxA to be upregulated in the Hfq/Crc-null strain (Table S6). The precise genes controlled by each of the different ECF-sigma factors upregulated in the Hfq-null strain are not known in many cases, although those coding for ECF-2 (FecI), ECF-5, ECF-7 (FiuI), ECF-9, ECF-15 and ECF-19 (IutY) are followed by genes that code for a ferric siderophore receptor or a heme receptor (Martínez-Bueno et al., 2002). The gene for ECF-16, which was also upregulated in the

present assays, is associated with a gene coding for a probable efflux system of unknown function.

Interestingly, the ECF-4 sigma factor, also known as PvdS or PfrI, showed elevated expression in the Hfq-null strain, as demonstrated by real-time RT-PCR (Table S8). However, both the RNA-seq and real-time RT-PCR assays indicated that its expression was very low, consistent with earlier reports showing that, in *P. aeruginosa*, PvdS expression is undetectable under iron-rich conditions such as those used here to culture the cells for the RNA-seq assays (Tiburzi et al., 2008). PvdS directs the expression of many genes involved in the synthesis of pyoverdine in *Pseudomonas syringae*, *P. aeruginosa*, and presumably in *P. putida* as well (Visca et al., 2002; Swingle et al., 2008; Edgar et al., 2017), including many of those for which the mRNA levels decreased upon inactivation of *hfq*. The increase detected in *pvdS* mRNA in the *P. putida* Hfq-null strain did not result in any greater expression of the pyoverdine-related genes under iron-replete conditions; it may be that the PvdS concentrations achieved were too low to efficiently compete for the RNA polymerase core.

Influence of Hfq and Crc on the production of pyoverdine under iron-limiting and iron-replete conditions

For the RNA-seq assays, the cells were cultured in minimal salts medium supplemented with a mixture of cations, including iron; this has been used by many research groups to study *P. putida*. The iron concentration of this medium, as measured by inductively coupled plasma mass spectrometry (ICP-MS), was found to be 84.5 ± 2.6 μM. This is a non-limiting concentration that allows for efficient growth (Molina et al., 2005). Since the lack of Crc/Hfq led to the reduced expression of many genes related to pyoverdine synthesis under these iron-replete conditions, experiments were performed to determine whether Crc or Hfq had any impact on the amount of pyoverdine produced under high (84.5 μM) or low (0.3 μM) iron concentrations. To this end, cells were cultured in M9

succinate medium containing either 84.5 or 0.3 μM iron in black, clear-bottomed microtiter plates, and the amount of pyoverdine produced followed by measuring fluorescence over time at 30°C. Growth (A_{600}) was also monitored to normalize the fluorescence values to the number of cells present. Both the wild type and the Crc-null strain produced a strong fluorescence signal when cultured under iron-limiting conditions (Fig. 3A,B; continuous lines). The signal detected was much lower when iron was present in excess (Fig. 3A,B; dashed lines). Strain KT2440*pvdD*, which is unable to synthesize pyoverdine and was used as control, rendered a very low fluorescence signal. Under iron-replete conditions, the fluorescence signal recorded for the wild type and Crc-null strains was essentially the same (Fig. 3B). This indicates that the lesser expression of the pyoverdine production genes detected by the RNA-seq in the Crc-null strain is insufficient to generate a visible phenotype. The Hfq-null strain behaved differently. Under iron limiting conditions, the lack of Hfq led to a strong reduction in fluorescence (Fig. 3A), suggesting that pyoverdine production was much reduced compared to the wild type strain. At high iron concentrations, the lack of Hfq also reduced fluorescence production (Fig. 3B). Pyoverdine production was restored upon introduction into strain KT2440Δ*hfq* of a plasmid bearing a wild type *hfq* gene (plasmid pHFQ, see Fig. 3C).

Similar results were obtained when pyoverdine production was assayed in agar plates containing increasing concentrations of 2,2'-dipirydyl, a compound that chelates iron leading to iron deprivation (Watson et al., 2010). Under high iron conditions, neither the wild type nor the mutant strains tested produced pyoverdine at detectable levels. However, the addition of 1.2 mM 2,2'-dipirydyl led to the secretion of the yellow/green pigment characteristic of pyoverdine. This was much more abundant in the wild type and Crc-null strains than in the Hfq-null strains (Fig. 3D). At higher 2,2'-dipirydyl concentrations, the Hfq-deficient strains did not grow, presumably because they were unable to scavenge enough iron from the medium. The wild type and Crc-null strains, in contrast, still produced pyoverdine and survived (not shown).

Overall, the present results indicate that when Hfq is lacking, less pyoverdine is produced than in the wild type strain. Even so, the absence of Hfq had little effect on the intracellular iron concentration, as measured by ICP-MS, either under high or low iron conditions (Fig. 4). Indeed, the cells were able to accumulate iron intracellularly at concentrations higher than those present in the growth medium. The ability to accumulate iron has also been observed in *P. aeruginosa* (Cunrath et al., 2016). It is at present unclear how the Hfq-null strain, which produces much less pyoverdine than the wild type strain, manages to accumulate as much iron as the wild type under low iron conditions. Perhaps the low amounts of pyoverdine produced are enough to achieve this goal. The pyoverdine receptor FpvA was downregulated in the mutant strain. However, several other siderophore receptors were upregulated. Many of these are likely involved in the uptake of xenosiderophores that are not present in the growth medium used, but it cannot be discarded that one or more of them can also scavenge pyoverdine. The uptake of reduced Fe^{2+} is unlikely, given that cells were cultivated under highly aerobic conditions and transport systems for the ferrous iron similar to those found in *P. aeruginosa* (Cartron et al., 2006) do not seem to be present in *P. putida* KT2440. An alternative possibility is that the Hfq-null strain can secrete heme or citrate as an iron-scavenging system.

The precise mechanism by which the absence of Hfq leads to a reduction in pyoverdine production is currently unclear, but it might be due to a combination of factors. One of these might be related to the IscR global regulator. In many bacteria, including *E. coli* and pseudomonads, the *isc* genes are involved in the maturation of iron-sulphur clusters, which are key components of the active centres of many enzymes. In *E. coli*, the expression of the *isc* genes is repressed by the IscR transcriptional regulator in response to high levels of these clusters (Schwartz et al., 2001), as well as by the iron-responsive sRNA *rhyB* (Desnoyers et al., 2009). Interestingly, the increased expression of IscR in *P. aeruginosa* carrying a multicopy plasmid with *iscR* increases the total iron content of the cells and reduces siderophore production (Romsang et al., 2014). In the present work, the mRNA levels of *iscR* (PP_0841) in the *P. putida* Hfq/Crc-null strain were >5-fold higher

than in the wild type strain (Table S3). In the Hfq-null strain a 2.96-fold increase was detected (FDR<10^{-6}), value that is just below the fold-change filter imposed, precluding the gene from the list of those upregulated. These results were confirmed by real-time RT-PCR (Table S8). It is likely, therefore, that the increase in the IscR concentration that occurs when Hfq is lacking leads to a concomitant reduction in pyoverdine production.

Influence of Hfq/Crc on the expression and levels of the PrrF1 and PrrF2 sRNAs

As mentioned above, the PrrF1 and PrrF2 sRNAs participate in maintaining iron homeostasis in *P. aeruginosa*. These have a role similar to that of *E. coli* RhyB sRNA, which acts by pairing to complementary regions in target mRNAs, inhibiting their translation and triggering their degradation by RNases (Masse and Gottesman, 2002; Massé et al., 2003; Geissmann and Touati, 2004). The *E. coli* Hfq protein binds to RhyB, facilitating its pairing to target mRNAs and preventing its degradation by RNases (Massé et al., 2003). In *P. aeruginosa*, the genes coding for PrrF1 and PrrF2 are located in tandem, and can be transcribed either as two independent sRNAs or as a single larger sRNA named PrrH (Wilderman et al., 2004; Oglesby-Sherrouse and Vasil, 2010). The expression of these sRNAs is repressed by Fur in the presence of high iron concentrations. Genes such as *sdhABCD* (succinate dehydrogenase), *bfrB* (bacterioferritin B) and *katA* (catalase) have been proposed regulated by PrrF1 and PrrF2 (Wilderman et al., 2004).

PrrF1 and PrrF2 have also been localized in *P. putida*, although they are not located in tandem; PrrH is not, therefore, produced in this species (Wilderman et al., 2004; D'Arrigo et al., 2016). A detailed characterization of their regulation and influence in *P. putida* has been lacking. The precise 5'-ends of *P. putida* PrrF1 and PrrF2 were determined by primer extension assays (Fig. 5). The start of PrrF1 was found to be 15 nt downstream of that proposed earlier on the basis of RNA-seq analyses (D'Arrigo et al., 2016), while the 5'-end of PrrF2 was found 67 nt downstream of that previously proposed.

The start sites were clearly preceded by consensus sequences for σ^{70}-RNA polymerase in the -35 and -10 regions of both promoters. The use of the Virtual Footprint tool (http://www.prodoric.de/vfp/; Münch et al., 2005) predicted the presence of a Fur box in both promoters, overlapping the -10 consensus region (Fig. 5). The sequence similarity of these putative Fur boxes to the 19 nt consensus described for Gram negative bacteria (Escolar et al., 1999) was 12 out of 19 positions for P_{prrF1}, and 13 out of 19 for P_{prrF2}. Both Fur boxes were 15 out of 19 bp identical to the respective ones in *P. aeruginosa* (Fig. S4). This suggests that Fur might regulate the expression of these two promoters according to iron availability, as proposed for *P. aeruginosa* (Wilderman et al., 2004). The end of the two sRNAs was sought by combining the reported approximate size of these sRNAs (D'Arrigo et al., 2016) with the output obtained from the ARNold software tool, which finds Rho-independent terminators (http://rna.igmors.u-psud.fr/toolbox/arnold/). This suggested that the two sRNAs are very similar in size (PrrF1, ~116 nt; PrrF2, ~114 nt; see Fig. 5) and that they share extensive nucleotide similarity (80%).

A Northern blot assay using probes directed towards PrrF1 or PrrF2 rendered (in both cases) a single band of the expected size when using RNA obtained from cells cultured under low iron conditions. When iron was plentiful the band was clearly less intense (Fig. 6A,B). The pattern was similar for both probes. The intensity of the bands was quantified in three independent assays using the PrrF2 probe which, due to its extensive similarity to PrrF1, likely hybridizes with both sRNAs. In the wild type strain, the transcript detected was at least 4-fold less abundant when iron was in excess (P<0.005; Fig. 6C). Similar assays performed with the Crc-null, Hfq-null and Crc-Hfq-null strains showed that the absence of Crc had no influence on the abundance of PrrF1-F2, while the absence of Hfq led to a significant reduction in the sRNAs under low iron conditions (Fig. 6C). This suggests that Hfq affects the transcription or the stability of these sRNAs.

The possible influence of iron and Hfq on the activity of promoters P_{PrrF1} and/or P_{PrrF2} was analysed using transcriptional fusions involving the *lacZ* reporter gene. When cells were cultivated in aerated flasks containing M9 succinate medium, the activity of promoter

P_{PrrF1} was greater under iron-limiting (0.3 μM) than under iron-replete (84.5 μM) conditions, although the difference was small (Fig. 7A). The influence of iron on the activity of promoter P_{PrrF2} was much more pronounced (Fig. 7B). In fact, at mid-exponential phase and under high iron conditions, the activity of P_{PrrF2} was about 6-fold lower than that of P_{PrrF1}, a difference that decreased to only 2-fold when iron was lacking. Therefore, promoter P_{PrrF2} is strongly repressed in the presence of iron, while the response of P_{PrrF1} to iron is much less strong. This suggests that the latter promoter might respond to other, unknown signals.

The inactivation of the *crc* and/or *hfq* genes had no influence on the activity of promoters P_{PrrF1} and P_{PrrF2} (Fig. 7C,D). This is in line with the observation that the inactivation of *crc* or *hfq* did not affect the amounts of Fur protein present (according to the iTRAQ assays), or the amount of iron in the cells (Fig. 4). Therefore, the smaller amounts of PrrF1 and/or PrrF2 sRNAs observed in the Hfq-null strain suggest that these sRNAs may be less stable when Hfq is lacking, presumably because Hfq can bind to and protect them from RNases. The low abundance of these sRNAs in the Hfq-null strain prevented their half-lives from being accurately determined. The finding that inactivation of the *hfq* gene in *P. putida* does not affect significantly *fur* mRNA levels or the amount of Fur protein detected (Arce-Rodríguez et al., 2016, and this work) contrasts with the results showing that Hfq indirectly regulates *fur* expression in *E. coli* (Massé et al., 2003). This highlights that the way in which Hfq controls iron metabolism differs in these two species.

Conclusions

Catabolite repression in pseudomonads mainly relies on the ability of Crc and Hfq to form stable tripartite complexes at target mRNAs, inhibiting their translation (Moreno et al., 2009b; Madhushani et al., 2015; Moreno et al., 2015; Sonnleitner et al., 2017). However, the results presented here support the view that these proteins participate in other,

important regulatory processes, such as iron homeostasis, following a different strategy. In iron homeostasis, Hfq is the main protagonist, the function of Crc being to facilitate control of the amount of free Hfq in the cell. Crc can perform this task by being instrumental in the formation of stable Crc-Hfq-RNA complexes with the regulatory CrcZ and CrcY sRNAs, as well as in the production of these sRNAs. The results presented suggest that when most Crc molecules are sequestered by CrcZ/CrcY, a significant amount of free Hfq remains to perform its role as a riboregulator, most likely acting on a range of sRNAs. It should be recalled that the total amount of Crc and Hfq (free molecules plus those sequestered by CrcZ/CrcY) varies little under different physiological conditions, while that of CrcZ and CrcY changes substantially (Sonnleitner et al., 2006; Sonnleitner et al., 2009; Moreno et al., 2015).

Iron homeostasis in *Pseudomonas* relies on a number of regulatory elements, with the PrrF1 and PrrF2 sRNAs playing a key role (reviewed in Cornelis et al., 2009; Llamas et al., 2014). The present finding that the levels of these sRNAs decrease significantly in a mutant strain lacking Hfq suggests that at least part of the influence of Hfq on iron homeostasis derives from its ability to control the levels of these sRNAs, probably by protecting them from degradation by RNases. Certainly, the stability of the *E. coli* RyhB sRNA, which has a role similar to that of the PrrF1-F2 sRNAs, is compromised when Hfq is lacking (Massé et al., 2003). However, Hfq would also influence other elements of iron metabolism in *Pseudomonas*, for example the levels of the IscR regulator, as discussed above.

The presence of a link between iron and carbon metabolism makes sense since several key enzymes involved in the assimilation of carbon compounds require iron as cofactor. In particular, succinate dehydrogenase, a key enzyme in the assimilation of succinate (the carbon source used in this work), is a multimeric complex that contains three iron-sulphur clusters ([2Fe-2S], [4Fe-4S], and [3Fe-4S]) and a heme cofactor. It therefore has significant iron demands. In addition, it has long been known that the amount of siderophores produced by pseudomonads varies according to the carbon source used,

which likely reflects the iron needs of the enzymes required by the cell to assimilate the carbon available (Hohnadel and Meyer, 1986). The participation of Hfq in iron homeostasis, together with its reported influence on stress tolerance, catabolite repression and quorum sensing (Sonnleitner et al., 2006; Sonnleitner and Blasi, 2014; Moreno et al., 2015; Arce-Rodríguez et al., 2016), highlights the importance of this riboregulator in the fine-tuning of cell physiology in pseudomonads.

Experimental procedures

Bacterial strains and culture media

The strains used in this work were *E. coli* DH5α (Woodcock et al., 1989), *E. coli* HB101 (pRK600) (Kessler et al., 1992), *P. putida* KT2440 (Franklin et al., 1981), *P. putida* KT2440Δ*hfq* (Arce-Rodríguez et al., 2016), *P. putida* KTVC (a *crc::aacC1* derivative of strain KT2440; this work), and the double mutant *P. putida* KTHC (KT2440Δ*hfq crc::aacC1*; this work). *Pseudomonas putida* KTVC and KTHC were derived from *P. putida* KT2440 and KT2440Δ*hfq* respectively; the *crc* gene was replaced by an inactive *crc::aacC1* via allele-by-allele exchange using plasmid pCRC10Gm (Moreno et al., 2007). Strain KT2440*pvdD*, which is a KT2440 derivative with a mini-Tn5 insertion in *pvdD* (PP_4219), belongs to a knockout library described earlier (Molina-Henares et al., 2010).

E. coli strains were grown at 37°C and *P. putida* strains at 30ºC. Cells were cultivated in complete LB medium (10 g/L tryptone, 5 g/L yeast extract, 10 g/L NaCl) or in M9 minimal salts medium (Sambrook and Russell, 2001) supplemented with trace elements (Bauchop and Eldsen, 1960); the composition of this medium is 42.4 mM Na_2HPO_4, 22 mM KH_2PO_4, 8.6 mM NaCl, 18.7 mM NH_4Cl, 25 μM $CaCO_3$, 1.2 μM $CoSO_4$, 1.3 μM $CuSO_4$, 42.7 μM $FeSO_4$, 0.4 μM H_3BO_3, 776 μM HCl, 333 μM MgO, 38.1 μM $MnSO_4$, 6.25 μM $ZnSO_4$. In this work, iron concentration was adjusted to either 84.5 μM (high Fe condition) or to 0.3 μM (low Fe condition), in this latter case by replacing the

Fe_2SO_4 for $(NH_4)_2SO_4$ at the same molar concentration. Succinate (30 mM) was added as the carbon source.

When needed, antibiotics were added at the following concentrations: kanamycin 50 µg/mL, gentamicin 40 µg/mL, ampicillin 100 µg/mL, streptomycin 50 µg/mL. Cell growth was monitored by measuring turbidity at 600 nm.

Plasmids

To complement the Δ*hfq* mutation in *trans*, a 669 bp DNA fragment including the *hfq* gene and its own promoter was PCR amplified from *P. putida* KT2440 chromosome using oligonucleotides HfqComp-few-EcoRI and HfqComp-rv-HindIII (Table S9), and cloned into plasmid pGEM-T Easy (Promega). The insert was excised with NotI and introduced at the NotI site of plasmid pSEVA421 (Martínez-García et al., 2015a), obtaining plasmid pHFQ. After checking the integrity of the *hfq* sequence by DNA sequencing, plasmid pHFQ was introduced into *P. putida* strain KT2440Δ*hfq*.

To obtain transcriptional fusions of promoters *PprrF1* and *PprrF2* to the *lacZ* reporter gene, 159 bp and 292 bp DNA fragments containing, respectively, the promoters for the *prrF1* and *prrF2* genes, were PCR-amplified using *P. putida* KT2440 genomic DNA as a template and the oligonucleotide pairs PprrF1-fw and PprrF1-rv, or PprrF2-fw PprrF2B-rv (Table S9). These DNA fragments were cloned between the HindIII and BamHI sites of plasmid pSEVA225 (Martínez-García et al., 2015a) to generate a transcriptional fusion to the *lacZ* reporter gene. The plasmids obtained, named pPprrF1 and pPprrF2, respectively, were transformed into *P. putida* KT2440 and its by-products KT2440*Δhfq,* KTVC and KTHC.

RNA purification

To obtain total RNA for use in real-time RT-PCR assays, cells were grown at 30ºC in aerated flasks in M9 minimal salts medium containing 30 mM succinate as the carbon source. At mid-exponential phase (A_{600}=0.6), 20 ml samples were collected, harvested by

centrifugation, and frozen at -70ºC. Total RNA was purified from cell pellets using the RNeasy RNA purification kit (QIAGEN). Purified RNA was treated with RNase-free DNase I (TURBO DNA-free, Ambion), as indicated by the manufacturer. RNA integrity was analysed by agarose gel electrophoresis. The absence of DNA in the RNA preparations was tested by real-time PCR using primers for *rpoN* (Morales et al., 2006). Since this method is of no use for RNAs smaller than 300–400 bp, an alternative procedure was used when sRNAs were the targets of analysis. The cells were collected by centrifugation from 40 ml of culture and RNA purification then performed using the TRIzol Max Bacterial Isolation Kit (Ambion), following the manufacturer's instructions.

Real-time RT-PCR

For real-time RT-PCR assays, RNA preparations obtained from three independent cultures (three biological replicas) were used. RNA was transformed into cDNA using the cDNA Archive Kit (Applied Biosystems). Real-time PCR was performed as previously described (Morales et al., 2006; Moreno et al., 2010) using the $2^{-\Delta\Delta Ct}$ method (Livak and Schmittgen, 2001) and the primers listed in Table S9. The results were normalized relative to those obtained for the *rpoN* gene, the expression of which remains constant throughout the growth curve under a range of growth conditions (Cases et al., 1996; Yuste et al., 2006).

RNA-seq assays

P. putida strains KT2440, KT2440Δ*hfq*, KTVC, and the double mutant KTHC, were cultured in M9 minimal salts medium containing succinate as the carbon source to a turbidity of 0.6. Cells were collected by centrifugation at 4°C and total RNA purified using the RNeasy kit (QIAGEN). It was then treated with the RNase-free DNase Set Kit (QIAGEN) to completely eliminate all residual DNA. RNA quality was examined using an Agilent 2100 Bioanalyzer (Agilent Technologies). RNA-seq library construction and deep-sequencing were carried out by the Genomics Unit at the *Parque Científico de Madrid* (Madrid, Spain). Ribosomal RNA was eliminated using the Ribo-Zero rRNA Removal Kit

for bacteria (Illumina). Directional (strand-specific) libraries were constructed using the Illumina mRNA Sequencing Sample Preparation Kit (TruSeq) and sequenced in single-end-read format (1x150) using the Illumina HiSeqTM 2000 system (Illumina). To obtain a homogeneous sequence dataset, short reads were quality-checked with FastQC (Babraham Bioinformatics; http://www.bioinformatics.babraham.ac.uk/projects/fastqc). These were then aligned against the *P. putida* KT2440 genome (NCBI reference sequence NC_002947.3) using Bowtie2 software (Langmead and Salzberg, 2012) employing the default parameters. About 3 million reads were obtained for each sample, 96-99% of which could be aligned with the *P. putida* KT2440 chromosome. Most were unique hits (>92.45% of total reads). Sorting and indexing of the alignment files (.bam files) was performed using the SAMtools software package (Li et al., 2009). The genomic alignment of the reads was visualized using the IGV browser (Robinson et al., 2011). Unique aligned reads were assigned to bacterial genes (quantification) with the HTSeq-count function of HTSeq Python package (Anders et al., 2015). The differential expression of genes between samples was quantified using the Bioconductor edgeR package (Robinson et al., 2010), employing the default parameters. Since only one sample form each strain was analysed by RNA-seq, the statistical significance of the results was estimated using the recommended imputed dispersion value of 0.1^2 (Bioconductor edgeR manual; Robinson et al., 2010). This allowed false discovery rates (FDR) to be estimated. The FIESTA viewer was used to filter differentially expressed genes (Oliveros, 2007). Results of interest were confirmed by independent real-time RT-PCR assays. The complete raw dataset for the RNA-seq assays were deposited at the NCBI's Gene Expression Omnibus site (http://www.ncbi.nlm.nih.gov/geo) under accession code GSE110803.

Quantitative analysis of proteomes by mass spectrometry (MS) using isobaric tagging relative and absolute quantitation (iTRAQ)

Proteomic analyses were performed at the CNB-CSIC proteomics facility (Madrid, Spain; http://proteo.cnb.csic.es/proteomica/). Briefly, *P. putida* KT2440, KT2440Δ*hfq*, KTVC and

the double mutant KTHC were cultured in M9 minimal medium with succinate as the carbon source. At mid-exponential phase (A_{600}=0.6), 20 ml of culture were withdrawn and the cells harvested by centrifugation at 4°C. The pellets were resuspended in 2 ml of a lysis buffer containing 20 mM Tris, 7 M urea, 2 M thiourea, 5% (w/v) 3-((3-cholamidopropyl)dimethylammonium)-1-propanesulfonate (CHAPS) and protease inhibitor cocktail tablets (Roche). Cells were disrupted by sonication on ice and the debris eliminated by centrifugation at 14,000 rpm for 30 min at 4°C. Proteins in the supernatant were precipitated with methanol/chloroform (Wessel and Flugge, 1984) and resuspended in 160 μl of a buffer containing 7 M urea, 2 M thiourea and 100 mM tetraethylammonium bromide. For iTRAQ tagging, 40 μg of proteins from each sample were digested overnight at 37°C with 4 μg of trypsin (Sigma-Aldrich). The resulting peptides were labelled for 2 h with iTRAQ tags (AB Sciex; one tag for each strain, 8-plex procedure) according to the manufacturer's recommendations. The labelled samples were mixed and cleaned through a C18 SEP-PAK column. An amount of sample equivalent to a total of 1 μg of labelled peptides was then analysed by liquid chromatography/mass spectrometry in an AB Sciex TRIPLE Q-TOF mass spectrometer.

Protein identification and the analysis of protein differential expression were performed by Proteobotics S.L. (Madrid, Spain). Briefly, MS/MS spectra were exported to *mgf* format using Peak View v1.2.0.3 and searched using Mascot Server 2.5.1, OMSSA 2.1.9, X!TANDEM 2013.02.01.1, and Myrimatch 2.2.140, against a composite target/decoy database built from the 5313 *P. putida* KT2440 sequences at Uniprot Knowledgebase (November 2015), together with commonly occurring contaminants. Search engines were configured to match potential peptide candidates with a mass error tolerance of 25 ppm and fragment ion tolerance of 0.02Da, allowing for up to two missed tryptic cleavage sites and a maximum isotope error (^{13}C) of 1, considering fixed methyl-methane-thiosulphonate (MMTS) modification of cysteine and variable oxidation of methionine, pyroglutamic acid from glutamine or glutamic acid at the peptide N-terminus, and modification of lysine and

peptide N-terminus with Tandem Mass Tags (TMT) 6-plex reagents. Score distribution models were used to compute peptide-spectrum match *p*-values (Ramos-Fernández et al., 2008), and spectra recovered by a FDR ≤ 0.01 (peptide-level) filter were selected for quantitative analysis. Approximately 1% of the signals with the lowest quality were removed prior to further analysis. Differential regulation was measured using linear models (López-Serra et al., 2014), and statistical significance was measured using *q*-values (FDR). All analyses were conducted using software from Proteobotics (Madrid, Spain). Proteins showing an abundance change of ≥1.4 fold ($\log_2$ of 0.49), and a *q*-value of ≤0.05, were considered differentially expressed, as recommended earlier (Koul et al., 2014).

Determination of bacterial cell iron content (ICP-MS)

When cultures reached a turbidity of 0.6 (A_{600}), cells from 15 ml samples were collected by centrifugation, dissolved in 20% nitric acid, and boiled. The iron content of the samples was determined by ICP-MS at the *Servicio Interdepartamental de Investigación*, belonging to the *Universidad Autónoma de Madrid* (Spain). The raw data (in μg/L) were normalized relative to the number of cells present in the sample (absorbance at 600 nm). The iron concentrations provided are the mean of two biological replicates.

Pyoverdine detection

Pyoverdine production was determined by fluorescence spectroscopy (excitation 405 nm, emission 460 nm), normalizing the fluorescence value obtained to the cell density of the culture ($A_{600\ nm}$), essentially as previously described (Baysse et al., 2001; Guillon et al., 2012). Cells were cultured to stationary phase in LB medium, washed extensively three times in minimal salts M9 medium lacking iron, and inoculated into M9 medium containing either 84.5 or 0.3 μM iron to a turbidity of 0.03 (A_{600}). 150 μl of the suspension were transferred (in triplicate) to 96-well black microtiter plates with clear flat bottoms (Costar). These were then incubated at 30°C with agitation in a Tecan microplate reader, measuring

fluorescence and cell growth (A_{600}) every 10 min for 18 h. Results are expressed as the mean of three technical replicates. Two independent assays were performed. A mutant strain unable to synthesize pyoverdine (KT2440*pvdD*) was used as control.

To detect pyoverdine production in solid media, cells were cultured as indicated above, and 10 μl deposited on minimal salts M9 medium agar plates (1.5% agar) containing 84.5 μM iron, 30 mM succinate, and increasing concentrations of 2,2'-dipyridyl. The plates were incubated at 30°C for 48 h and pyoverdine production visualized by illumination with white light.

Northern blots

To generate an RNA probe against the PprrF1 and PrrF2 sRNAs, a DNA segment including the complete sRNA region was PCR amplified using primers prrF1-dir-EcoRI and prrF1-rev-PstI, or prrF2-dir-EcoRI and prrF2-rev-PstI (Table S9), which include restriction sites for EcoRI and PstI endonucleases. The resulting DNA fragments were digested with EcoRI and PstI and cloned into plasmid pSPT18 (Roche), to obtain plasmids pSPT18-prrF1 and pSPT18-prrF2. These were linearized with EcoRI and employed as a template for an *in vitro* transcription reaction using the DIG RNA labelling kit (Roche) and SP6 RNA polymerase. To generate a probe against the 5S ribosomal RNA, a DNA fragment corresponding to the gene specifying the 5S RNA was PCR-amplified using primers 5S-HindIII-fw and 5S-EcoRI-rv (Table S9), and the resulting fragment cloned between the HindIII and EcoRI sites of plasmid pSPT18, generating plasmid pSPT18-5S. This plasmid was linearized with HindIII and used as a template for an *in vitro* transcription reaction with T7 RNA polymerase as indicated above (Hernández-Arranz et al., 2016).

For Northern blots, 2.5 μg total RNA purified from the indicated strains were resolved by electrophoresis on a 6% polyacrylamide gel containing 7 M urea and transferred to a Nylon Hybond N+ membrane (GE Healthcare Biosciences) with a semi-dry transfer unit (Trans-blot SD. Bio-Rad; 400 mA, 1 h). Membranes were UV-crosslinked and hybridized with a mixture of DIG-labelled probes against PrrF1-F2 and 5S. Bands were detected

using the DIG Luminescent Detection Kit (Roche) and visualized by exposure to Agfa X-ray film, or with a Chemidoc device (BioRad). The latter was used to quantify band intensity. The results shown are the mean of three independent assays.

Identification of the prrF1 *and* prrF2 *transcription start sites by primer extension*

The oligonucleotides used as primers for the extension reactions, PE PprrF1-INV and PE PprrF2B-INV (see Table S1), were end-labelled with [γ-^{32}P]ATP and T4 polynucleotide kinase. 25 μg of RNA (obtained as indicated above) were mixed with 10 pmol of the end-labelled primer and heated (80ºC, 5 min). The oligonucleotide was allowed to anneal to the RNA by incubation (23ºC, 5 min). Primer extension was performed with 200 U SuperScript III (Promega) at 55ºC, as indicated by the supplier. The extended cDNA products were analysed by electrophoresis on a denaturing 6% urea-polyacrylamide gel, in parallel with a DNA sequence ladder obtained by the chemical sequencing (Maxam and Gilbert, 1980) of a DNA fragment obtained via PCR using oligonucleotides PE PprrF1-DIR and PE PprrF1-INV (the latter labelled with [γ-^{32}P]ATP using T4 polynucleotide kinase), employing *P. putida* chromosomal DNA as template. The gel was dried, exposed to a phosphorimager screen and visualized using a Personal Molecular Imager (BioRad).

Assay for β-galactosidase

Overnight cultures in minimal salts M9 medium containing succinate as the carbon source were centrifuged and washed three times with M9 salts medium (i.e., lacking the trace elements solution, and therefore iron), and finally diluted to a turbidity (A_{600}) of 0.05 in fresh M9 succinate medium containing the amount of iron indicated in each assay. Cells were allowed to grow at 30°C with vigorous aeration; aliquots were taken at various times and β-galactosidase activity measured using o-nitrophenyl-β-D-galactoside as a substrate (Miller, 1972). Three independent assays were performed.

Acknowledgements

We are grateful to V. de Lorenzo and E. Duque for providing the *P. putida* Hfq-null and PvdD-null strains, respectively, and to J.C. Oliveros for help in the design and interpretation of RNA-seq assays. DS-H received a predoctoral fellowship from the Spanish Ministry of Science and Competitiveness (MINECO). This work was funded by grant BIO2015-66203-P (AEI/FEDER, UE).

Figure Legends

Figure 1. Number of genes for which RNA levels were altered by more than 3-fold in strains KTVC (Crc-null, green circle), KT2440Δ*hfq* (Hfq-null, blue circle) and KTHC (Crc-null, Hfq-null, pink circle), compared to the wild type (KT2440), as deduced in RNA-seq assays. Genes affected in more than one mutant strain are indicated in the intersections of the circles. Cells were cultivated in M9 minimal salts medium containing succinate as the carbon source. The most important functions or genes affected in each mutant strain are indicated on the right.

Figure 2. Effect of Hfq on the expression of genes involved in iron metabolism. (**A**) Simplified diagram of the synthesis, export and uptake of pyoverdine in *Pseudomonas*, and the involvement of the Fur protein and the PrrF1 and PrrF2 sRNAs in the regulation of iron homeostasis. The diagram is based on what it is known for different pseudomonads (see Cornelis et al., 2009; Cornelis, 2010; Schalk and Guillon, 2013; Llamas et al., 2014; Schalk and Cunrath, 2016). The colours indicate the expression trend in the Hfq-null strains (red, higher expression, green, lower expression) (**B**) Genes related to the synthesis, export, uptake and regulation of ferric siderophores, or to iron storage, that showed either increased (in red) or reduced (in green) RNA levels in the Crc-null (labelled as “1”), Hfq-null (labelled as “2”), or Crc/Hfq-null (labelled as “3”) strains relative to the wild type.

Figure 3. Effect of Crc and Hfq on the production of pyoverdine. *Pseudomonas putida* KT2440 (wild type), KTVC (Crc-null), KT2440Δ*hfq* (Hfq-null), KTHC (Crc-null, Hfq-null), and KT2440*pvdD* (a PvdD-null stain unable to synthesize pyoverdine) were inoculated at a turbidity of 0.03 (A_{600}) in minimal salts M9 succinate medium containing either 84.5 or 0.3 μM iron, transferred to a 96-well black clear-bottomed microtiter plate, and allowed to grow at 30°C. The amount of pyoverdine produced was followed by measuring fluorescence

over time, as indicated in Experimental Procedures. Growth (A_{600}) was also monitored to normalize the fluorescence values relative to the turbidity of the cultures. (**A**). Fluorescence profiles (normalised to A_{600}) for cells cultured under high (scattered lines) or low (continuous lines) iron concentrations. (**B**) Enlarged view of the fluorescence profile observed under low iron conditions. (**C**) Complementation of the *hfq* mutation by a plasmid bearing a wild type copy of the *hfq* gene (plasmid pHFQ). *Pseudomonas putida* strains KT2440 (wt), KTVC (*crc*), KT2440Δ*hfq* (*hfq*) and KT2440Δ*hfq* containing plasmid pHFQ (*hfq*-pHFQ) were inoculated at a turbidity of 0.03 (A_{600}) in iron-deficient medium (0.3 μM iron); fluorescence was determined 4 hours later and normalised to A_{600}. Values are the average of three assays; the significance of the difference between the signal obtained for each strain relative to that of the wild type strain is indicated (one-way ANOVA; ***, *P*<0.001"; "ns", no significant difference). (**D**) Production of pyoverdine in agar plates. 10 μl of M9 succinate medium containing about 10^6 cells of the bacterial strains indicated above were spotted onto an M9 succinate medium agar plate containing 84.5 μM iron. Where indicated, 1.2 mM of 2,2'-dipyridyl (DPD) were added to chelate the iron. Plates were incubated at 30°C; pyoverdine production can be visualized as a yellow/green pigment surrounding the bacteria.

Figure 4. Total content of iron in cells. *Pseudomonas putida* KT2440 (wild type), KTVC (Crc-null), KT2440Δ*hfq* (Hfq-null) and KTHC (Crc-null, Hfq-null) were cultured in M9 succinate medium (MMScc) containing low (0.3 μM) or high (84.5 μM) iron concentrations. At mid exponential phase (A_{600}=0.6), the cells were collected and their iron concentration determined by ICP-MS as indicated in Experimental Procedures. The data obtained were normalized relative to the number of cells present in the sample (absorbance at 600 nm). The values indicated are the means of three biological replicates. The initial iron concentration of the growth medium used is indicated with a red line.

Figure 5. Identification of the promoters of the genes encoding the PrrF1 and PrrF2 sRNAs. (**A**, **B**) Location of the genes *prrF1* (**A**) and *prrF2* (**B**); the sequence of each sRNA is indicated in bold. The position of the transcription start site, as determined by primer extension (see C), is indicated by an arrow. The sequences at the -10 and -35 regions showing similarity to the consensus for the vegetative sigma factor are depicted, as are possible Rho-independent transcriptional terminators (stem-loops indicated by grey arrows), and a sequence showing similarity to the binding sequence of the Fur protein (red rectangle; for additional details, see Fig. S4). (**C**) Transcription start sites determined by primer extension, using RNA obtained from cells growing exponentially in M9 succinate medium containing 0.3 μM iron, and an appropriate end-labelled oligonucleotide (see Experimental Procedures). The size of the cDNA obtained was analysed in a denaturing urea-polyacrylamide gel; it was run side by side with a DNA sequence ladder obtained by the chemical sequencing of a 5'-end labelled DNA fragment (G+A reaction; indicated as "M"; Maxam and Gilbert, 1980). Arrows labelled "+1" indicate bands corresponding to the cDNA derived from the transcripts originated at promoters P_{prrF1} or P_{prrF2}.

Figure 6. Effect of Crc, Hfq and iron concentration on the levels of PrrF1 and PrrF2. Total RNA obtained from cells of strains KT2440 (wild type), KTVC (Crc-null), KT2440Δ*hfq* (Hfq-null) and KTHC (Crc-null, Hfq-null), cultured in M9 succinate medium containing low (0.3 μM) or high (84.5 μM) iron concentrations, was resolved by denaturing gel electrophoresis and transferred to a nitrocellulose membrane. The presence of PrrF1 and PrrF2 was determined by hybridization with appropriate probes. (**A**) Probe complementary to the complete PrrF1 sequence; RNA was obtained from cells cultured under low iron conditions. (**B**) Probe complementary to the complete PrrF2 sequence; RNAs obtained from cells cultured under low (L) or high (H) iron conditions. A probe complementary to 5S rRNA was included in all cases as a loading control. Note that since PrrF1 and PrrF2 are very similar in size and sequence, and the electrophoresis was performed in 7 cm-long gels, the assay was unable to distinguish them. (**C**) PrrF1-F2 abundance; data are the

means and standard deviations of three assays. The significance of the differences between the indicated pairs (deduced via the two-tailed *t*-test) is shown (**P*<0.1; ***P*<0.01; ****P*<0.001; "ns", no significant difference).

Figure 7. Effect of iron concentration (**A**, **B**), and of the Crc and Hfq proteins (**C**, **D**), on the activity of the P_{prrF1} and P_{prrF2} promoters. (**A**, **B**) *Pseudomonas putida* KT2440 containing plasmids pPprrF1 (contains a P_{prrF1}-*lacZ* transcriptional fusion) or pPprrF2 (contains a P_{prrF2}-*lacZ* transcriptional fusion) was cultured in M9 succinate medium containing high (84.5 μM, continuous line) or low (0.3 μM, dashed line) iron, and β-galactosidase activity measured at different times. The graph shows the values recorded as a function of cell growth (A_{600}). (**C**, **D**) *Pseudomonas putida* KT2440 (wild type), KTVC (Crc-null), KT2440Δ*hfq* (Hfq-null) and KTHC (Crc-null, Hfq-null) harbouring plasmids pPprrF1 or pPprrF2 were cultured in M9 succinate medium containing 0.3 μM iron, and their β-galactosidase activity measured. The figure shows the values observed in samples obtained at mid-exponential phase (A_{600} 0.6-0.8). Three independent assays were performed; the differences in promoter activity between the wild type and the mutant strains were not significant (one-way ANOVA).

References

Anders, S., Pyl, P.T., and Huber, W. (2015) HTSeq--a Python framework to work with high-throughput sequencing data. *Bioinformatics* **31**: 166-169.

Arce-Rodríguez, A., Calles, B., Nikel, P.I., and de Lorenzo, V. (2016) The RNA chaperone Hfq enables the environmental stress tolerance super-phenotype of *Pseudomonas putida*. *Environ Microbiol* **18**: 3309-3326.

Bastiaansen, K.C., Ibañez, A., Ramos, J.L., Bitter, W., and Llamas, M.A. (2014) The Prc and RseP proteases control bacterial cell-surface signalling activity. *Environ Microbiol* **16**: 2433-2443.

Bastiaansen, K.C., van Ulsen, P., Wijtmans, M., Bitter, W., and Llamas, M.A. (2015) Self-cleavage of the *Pseudomonas aeruginosa* Cell-surface Signaling Anti-sigma Factor FoxR Occurs through an N-O Acyl Rearrangement. *J Biol Chem* **290**: 12237-12246.

Bauchop, T., and Eldsen, S.R. (1960) The growth of microorganisms in relation to their energy supply. *J Gen Microbiol* **23**: 457-569.

Baysse, C., Matthijs, S., Pattery, T., and Cornelis, P. (2001) Impact of mutations in *hemA* and *hemH* genes on pyoverdine production by *Pseudomonas fluorescens* ATCC17400. *FEMS Microbiol Lett* **205**: 57-63.

Belda, E., van Heck, R.G., José López-Sánchez, M., Cruveiller, S., Barbe, V., Fraser, C. et al. (2016) The revisited genome of *Pseudomonas putida* KT2440 enlightens its value as a robust metabolic chassis. *Environ Microbiol* **18**: 3403-3424.

Cartron, M.L., Maddocks, S., Gillingham, P., Craven, C.J., and Andrews, S.C. (2006) Feo - transport of ferrous iron into bacteria. *Biometals* **19**: 143-157.

Cases, I., de Lorenzo, V., and Pérez-Martín, J. (1996) Involvement of sigma 54 in exponential silencing of the *Pseudomonas putida* TOL plasmid *Pu* promoter. *Mol Microbiol* **19**: 7-17.

Cornelis, P., and Matthijs, S. (2002) Diversity of siderophore-mediated iron uptake systems in fluorescent pseudomonads: not only pyoverdines. *Environ Microbiol* **4**: 787-798.

Cornelis, P., Matthijs, S., and Van Oeffelen, L. (2009) Iron uptake regulation in *Pseudomonas aeruginosa*. *Biometals* **22**: 15-22.

Cornelis, P. (2010) Iron uptake and metabolism in pseudomonads. *Appl Microbiol Biotechnol* **86**: 1637-1645.

Cornelis, P., Wei, Q., Andrews, S.C., and Vinckx, T. (2011) Iron homeostasis and management of oxidative stress response in bacteria. *Metallomics* **3**: 540-549.

Cunrath, O., Geoffroy, V.A., and Schalk, I.J. (2016) Metallome of *Pseudomonas aeruginosa*: a role for siderophores. *Environ Microbiol* **18**: 3258-3267.

D'Arrigo, I., Bojanovic, K., Yang, X., Holm Rau, M., and Long, K.S. (2016) Genome-wide mapping of transcription start sites yields novel insights into the primary transcriptome of *Pseudomonas putida*. *Environ Microbiol* **18**: 3466-3481.

Daniels, C., Godoy, P., Duque, E., Molina-Henares, M.A., de la Torre, J., Del Arco, J.M. et al. (2010) Global regulation of food supply by *Pseudomonas putida* DOT-T1E. *J Bacteriol* **192**: 2169-2181.

Desnoyers, G., Morissette, A., Prevost, K., and Masse, E. (2009) Small RNA-induced differential degradation of the polycistronic mRNA *iscRSUA*. *EMBO J* **28**: 1551-1561.

Edgar, R.J., Hampton, G.E., Garcia, G.P.C., Maher, M.J., Perugini, M.A., Ackerley, D.F., and Lamont, I.L. (2017) Integrated activities of two alternative sigma factors coordinate iron acquisition and uptake by *Pseudomonas aeruginosa*. *Mol Microbiol* **106**: 891-904.

Escolar, L., Pérez-Martín, J., and de Lorenzo, V. (1999) Opening the iron box: transcriptional metalloregulation by the Fur protein. *J Bacteriol* **181**: 6223-6229.

Fedral-Register (1982) Certified host-vector systems. p. 17197.

Ferrara, S., Carloni, S., Fulco, R., Falcone, M., Macchi, R., and Bertoni, G. (2015) Post-transcriptional regulation of the virulence-associated enzyme AlgC by the sigma(22) -dependent small RNA ErsA of *Pseudomonas aeruginosa*. *Environ Microbiol* **17**: 199-214.

Franklin, F.C., Bagdasarian, M., Bagdasarian, M.M., and Timmis, K.N. (1981) Molecular and functional analysis of the TOL plasmid pWWO from *Pseudomonas putida* and cloning of genes for the entire regulated aromatic ring *meta* cleavage pathway. *Proc Nat Acad Sci USA* **78**: 7458-7462.

García-Mauriño, S.M., Pérez-Martínez, I., Amador, C.I., Canosa, I., and Santero, E. (2013) Transcriptional activation of the CrcZ and CrcY regulatory RNAs by the CbrB response regulator in *Pseudomonas putida*. *Mol Microbiol* **89**: 189-205.

Geissmann, T.A., and Touati, D. (2004) Hfq, a new chaperoning role: binding to messenger RNA determines access for small RNA regulator. *EMBO J* **23**: 396-405.

Grenga, L., Chandra, G., Saalbach, G., Galmozzi, C.V., Kramer, G., and Malone, J.G. (2017) Analyzing the Complex Regulatory Landscape of Hfq - an Integrative, Multi-Omics Approach. *Front Microbiol* **8**: 1784.

Guillon, L., El Mecherki, M., Altenburger, S., Graumann, P.L., and Schalk, I.J. (2012) High cellular organization of pyoverdine biosynthesis in *Pseudomonas aeruginosa*: clustering of PvdA at the old cell pole. *Environ Microbiol* **14**: 1982-1994.

Hernández-Arranz, S., Moreno, R., and Rojo, F. (2013) The translational repressor Crc controls the *Pseudomonas putida* benzoate and alkane catabolic pathways using a multi-tier regulation strategy. *Environ Microbiol* **15**: 227-241.

Hernández-Arranz, S., Sánchez-Hevia, D., Rojo, F., and Moreno, R. (2016) Effect of Crc and Hfq proteins on the transcription, processing, and stability of the *Pseudomonas putida* CrcZ sRNA. *RNA* **22**: 1902-1917.

Hester, K.L., Lehman, J., Najar, F., Song, L., Roe, B.A., MacGregor, C.H. et al. (2000) Crc is involved in catabolite repression control of the *bkd* operons of *Pseudomonas putida* and *Pseudomonas aeruginosa*. *J Bacteriol* **182**: 1144-1149.

Hohnadel, D., and Meyer, J.M. (1986) Pyoverdine-Facilitated Iron Uptake Among Fluorescent Pseudomonads. In *Iron, Siderophores, and Plant Diseases; NATO ASI Series (Series A: Life Sciences)*. Swinburne, T.R. (ed): Springer, Boston, MA, pp. 119-129.

Kessler, B., de Lorenzo, V., and Timmis, K.N. (1992) A general system to integrate *lacZ* fusions into the chromosomes of gram-negative eubacteria: regulation of the *Pm* promoter of the TOL plasmid studied with all controlling elements in monocopy. *Mol Gen Genet* **233**: 293-301.

Koul, A., Vranckx, L., Dhar, N., Gohlmann, H.W., Ozdemir, E., Neefs, J.M. et al. (2014) Delayed bactericidal response of *Mycobacterium tuberculosis* to bedaquiline involves remodelling of bacterial metabolism. *Nat Commun* **5**: 3369.

La Rosa, R., de la Peña, F., Prieto, M.A., and Rojo, F. (2014) The Crc protein inhibits the production of polyhydroxyalkanoates in *Pseudomonas putida* under balanced carbon/nitrogen growth conditions. *Environ Microbiol* **16**: 278-290.

La Rosa, R., Nogales, J., and Rojo, F. (2015) The Crc/CrcZ-CrcY global regulatory system helps the integration of gluconeogenic and glycolytic metabolism in *Pseudomonas putida*. *Environ Microbiol* **17**: 3362-3378.

Langmead, B., and Salzberg, S.L. (2012) Fast gapped-read alignment with Bowtie 2. *Nat Methods* **9**: 357-359.

Li, H., Handsaker, B., Wysoker, A., Fennell, T., Ruan, J., Homer, N. et al. (2009) The Sequence Alignment/Map format and SAMtools. *Bioinformatics* **25**: 2078-2079.

Linares, J.F., Moreno, R., Fajardo, A., Martínez-Solano, L., Escalante, R., Rojo, F., and Martínez, J.L. (2010) The global regulator Crc modulates metabolism, susceptibility to antibiotics and virulence in *Pseudomonas aeruginosa*. *Environ Microbiol* **12**: 3196-3212.

Livak, K.J., and Schmittgen, T.D. (2001) Analysis of relative gene expression data using real-time quantitative PCR and the 2-ΔΔCt Method. *Methods* **25**: 402-408.

Llamas, M.A., Sparrius, M., Kloet, R., Jimenez, C.R., Vandenbroucke-Grauls, C., and Bitter, W. (2006) The heterologous siderophores ferrioxamine B and ferrichrome activate signaling pathways in *Pseudomonas aeruginosa*. *J Bacteriol* **188**: 1882-1891.

Llamas, M.A., Imperi, F., Visca, P., and Lamont, I.L. (2014) Cell-surface signaling in *Pseudomonas*: stress responses, iron transport, and pathogenicity. *FEMS Microbiol Rev* **38**: 569-597.

López-Serra, P., Marcilla, M., Villanueva, A., Ramos-Fernández, A., Palau, A., Leal, L. et al. (2014) A DERL3-associated defect in the degradation of SLC2A1 mediates the Warburg effect. *Nat Commun* **5**: 3608.

MacGregor, C.H., Wolff, J.A., Arora, S.K., Hylemon, P.B., and Phibbs, P.V., Jr. (1992) Catabolite repression control in *Pseudomonas aeruginosa*. In *Pseudomonas, molecular biology and biotechnology*. Galli, E., Silver, S., and Witholt, B. (eds). Washington, D.C: American Society for Microbiology, pp. 198-206.

Madhushani, A., Del Peso-Santos, T., Moreno, R., Rojo, F., and Shingler, V. (2015) Transcriptional and translational control through the 5'-leader region of the *dmpR* master regulatory gene of phenol metabolism. *Environ Microbiol* **17**: 119-133.

Martínez-Bueno, M.A., Tobes, R., Rey, M., and Ramos, J.L. (2002) Detection of multiple extracytoplasmic function (ECF) sigma factors in the genome of *Pseudomonas putida* KT2440 and their counterparts in *Pseudomonas aeruginosa* PAO1. *Environ Microbiol* **4**: 842-855.

Martínez-García, E., and de Lorenzo, V. (2011) Engineering multiple genomic deletions in Gram-negative bacteria: analysis of the multi-resistant antibiotic profile of *Pseudomonas putida* KT2440. *Environ Microbiol* **13**: 2702-2716.

Martínez-García, E., Aparicio, T., Goñi-Moreno, A., Fraile, S., and de Lorenzo, V. (2015a) SEVA 2.0: an update of the Standard European Vector Architecture for de-/re-construction of bacterial functionalities. *Nucleic Acids Res* **43**: D1183-1189.

Martínez-García, E., Jatsenko, T., Kivisaar, M., and de Lorenzo, V. (2015b) Freeing *Pseudomonas putida* KT2440 of its proviral load strengthens endurance to environmental stresses. *Environ Microbiol* **17**: 76-90.

Masse, E., and Gottesman, S. (2002) A small RNA regulates the expression of genes involved in iron metabolism in *Escherichia coli*. *Proc Natl Acad Sci USA* **99**: 4620-4625.

Massé, E., Escorcia, F.E., and Gottesman, S. (2003) Coupled degradation of a small regulatory RNA and its mRNA targets in *Escherichia coli*. *Genes Dev* **17**: 2374-2383.

Matthijs, S., Laus, G., Meyer, J.M., Abbaspour-Tehrani, K., Schafer, M., Budzikiewicz, H., and Cornelis, P. (2009) Siderophore-mediated iron acquisition in the entomopathogenic bacterium *Pseudomonas entomophila* L48 and its close relative *Pseudomonas putida* KT2440. *Biometals* **22**: 951-964.

Maxam, A.M., and Gilbert, W. (1980) Sequencing end-labeled DNA with base-specific chemical cleavages. *Methods Enzymol* **65**: 499-560.

Miller, J.H. (1972) *Experiments in molecular genetics*. Cold Spring Harbor, N.Y.: Cold Spring Harbor Laboratory.

Molina, M.A., Godoy, P., Ramos-González, M.I., Muñoz, N., Ramos, J.L., and Espinosa-Urgel, M. (2005) Role of iron and the TonB system in colonization of corn seeds and roots by *Pseudomonas putida* KT2440. *Environ Microbiol* **7**: 443-449.

Molina-Henares, M.A., de la Torre, J., García-Salamanca, A., Molina-Henares, A.J., Herrera, M.C., Ramos, J.L., and Duque, E. (2010) Identification of conditionally essential genes for growth of *Pseudomonas putida* KT2440 on minimal medium through the screening of a genome-wide mutant library. *Environ Microbiol* **12**: 1468-1485.

Morales, G., Linares, J.F., Beloso, A., Albar, J.P., Martínez, J.L., and Rojo, F. (2004) The *Pseudomonas putida* Crc global regulator controls the expression of genes from several chromosomal catabolic pathways for aromatic compounds. *J Bacteriol* **186**: 1337-1344.

Morales, G., Ugidos, A., and Rojo, F. (2006) Inactivation of the *Pseudomonas putida* cytochrome *o* ubiquinol oxidase leads to a significant change in the transcriptome and to increased expression of the CIO and *cbb3*-1 terminal oxidases. *Environ Microbiol* **8**: 1764-1774.

Moreno, R., Ruiz-Manzano, A., Yuste, L., and Rojo, F. (2007) The *Pseudomonas putida* Crc global regulator is an RNA binding protein that inhibits translation of the AlkS transcriptional regulator. *Mol Microbiol* **64**: 665-675.

Moreno, R., Martínez-Gomariz, M., Yuste, L., Gil, C., and Rojo, F. (2009a) The *Pseudomonas putida* Crc global regulator controls the hierarchical assimilation of amino acids in a complete medium: evidence from proteomic and genomic analyses. *Proteomics* **9**: 2910-2928.

Moreno, R., Marzi, S., Romby, P., and Rojo, F. (2009b) The Crc global regulator binds to an unpaired A-rich motif at the *Pseudomonas putida alkS* mRNA coding sequence and inhibits translation initiation *Nucleic Acids Res* **37**: 7678-7690.

Moreno, R., Fonseca, P., and Rojo, F. (2010) The Crc global regulator inhibits the *Pseudomonas putida* pWW0 toluene/xylene assimilation pathway by repressing the translation of regulatory and structural genes. *J Biol Chem* **285**: 24412-24419.

Moreno, R., Fonseca, P., and Rojo, F. (2012) Two small RNAs, CrcY and CrcZ, act in concert to sequester the Crc global regulator in *Pseudomonas putida*, modulating catabolite repression. *Mol Microbiol* **83**: 24-40.

Moreno, R., and Rojo, F. (2014) Features of pseudomonads growing at low temperatures: another facet of their versatility. *Environ Microbiol Rep* **6**: 417-426.

Moreno, R., Hernández-Arranz, S., La Rosa, R., Yuste, L., Madhushani, A., Shingler, V., and Rojo, F. (2015) The Crc and Hfq proteins of *Pseudomonas putida* cooperate in catabolite repression and formation of ribonucleic acid complexes with specific target motifs. *Environ Microbiol* **17**: 105-118.

Münch, R., Hiller, K., Grote, A., Scheer, M., Klein, J., Schobert, M., and Jahn, D. (2005) Virtual Footprint and PRODORIC: an integrative framework for regulon prediction in prokaryotes. *Bioinformatics* **21**: 4187-4189.

Nelson, K.E., Weinel, C., Paulsen, I.T., Dodson, R.J., Hilbert, H., Martins dos Santos, V.A. et al. (2002) Complete genome sequence and comparative analysis of the metabolically versatile *Pseudomonas putida* KT2440. *Environ Microbiol* **4**: 799-808.

Nikel, P.I., Martínez-García, E., and de Lorenzo, V. (2014) Biotechnological domestication of pseudomonads using synthetic biology. *Nat Rev Microbiol* **12**: 368-379.

Oglesby-Sherrouse, A.G., and Vasil, M.L. (2010) Characterization of a heme-regulated non-coding RNA encoded by the *prrF* locus of *Pseudomonas aeruginosa*. *PLoS One* **5**: e9930.

Oliveros, J.C. (2007). FIESTA@BioinfoGP. An interactive server for analysing DNA microarrays experiments with replicates. URL http://bioinfogp.cnb.csic.es/tools/FIESTA

Poblete-Castro, I., Becker, J., Dohnt, K., Dos Santos, V.M., and Wittmann, C. (2012) Industrial biotechnology of *Pseudomonas putida* and related species. *Appl Microbiol Biotechnol* **93**: 2279-2290.

Pusic, P., Tata, M., Wolfinger, M.T., Sonnleitner, E., Haussler, S., and Bläsi, U. (2016) Cross-regulation by CrcZ RNA controls anoxic biofilm formation in *Pseudomonas aeruginosa*. *Sci Rep* **6**: 39621.

Quiroz-Rocha, E., Moreno, R., Hernández-Ortiz, A., Fragoso-Jiménez, J.C., Muriel-Millán, L.F., Guzmán, J. et al. (2017) Glucose uptake in *Azotobacter vinelandii* occurs through a GluP transporter that is under the control of the CbrA/CbrB and Hfq-Crc systems. *Sci Rep* **7**: 858.

Ramos, J.L., Cuenca, M.S., Molina-Santiago, C., Segura, A., Duque, E., Gómez-García, M.R. et al. (2015) Mechanisms of solvent resistance mediated by interplay of cellular factors in *Pseudomonas putida*. *FEMS Microbiol Rev* **39**: 555-566.

Ramos-Fernández, A., Paradela, A., Navajas, R., and Albar, J.P. (2008) Generalized method for probability-based peptide and protein identification from tandem mass spectrometry data and sequence database searching. *Mol Cell Proteomics* **7**: 1748-1754.

Robinson, J.T., Thorvaldsdottir, H., Winckler, W., Guttman, M., Lander, E.S., Getz, G., and Mesirov, J.P. (2011) Integrative genomics viewer. *Nat Biotechnol* **29**: 24-26.

Robinson, M.D., McCarthy, D.J., and Smyth, G.K. (2010) edgeR: a Bioconductor package for differential expression analysis of digital gene expression data. *Bioinformatics* **26**: 139-140.

Rojo, F. (2010) Carbon catabolite repression in *Pseudomonas*: optimizing metabolic versatility and interactions with the environment. *FEMS Microbiol Rev* **34**: 658-684.

Romsang, A., Duang-Nkern, J., Leesukon, P., Saninjuk, K., Vattanaviboon, P., and Mongkolsuk, S. (2014) The iron-sulphur cluster biosynthesis regulator IscR contributes to iron homeostasis and resistance to oxidants in *Pseudomonas aeruginosa*. *PLoS One* **9**: e86763.

Sambrook, J., and Russell, D.W. (2001) *Molecular cloning: a laboratory manual*. Cold Spring Harbor, N.Y.: Cold Spring Harbor Laboratory.

Schalk, I.J. (2008) Metal trafficking via siderophores in Gram-negative bacteria: specificities and characteristics of the pyoverdine pathway. *J Inorg Biochem* **102**: 1159-1169.

Schalk, I.J., and Guillon, L. (2013) Fate of ferrisiderophores after import across bacterial outer membranes: different iron release strategies are observed in the cytoplasm or periplasm depending on the siderophore pathways. *Amino Acids* **44**: 1267-1277.

Schalk, I.J., and Cunrath, O. (2016) An overview of the biological metal uptake pathways in *Pseudomonas aeruginosa*. *Environ Microbiol* **18**: 3227-3246.

Schwartz, C.J., Giel, J.L., Patschkowski, T., Luther, C., Ruzicka, F.J., Beinert, H., and Kiley, P.J. (2001) IscR, an Fe-S cluster-containing transcription factor, represses expression of *Escherichia coli* genes encoding Fe-S cluster assembly proteins. *Proc Natl Acad Sci USA* **98**: 14895-14900.

Sevilla, E., Silva-Jiménez, H., Duque, E., Krell, T., and Rojo, F. (2013) The *Pseudomonas putida* HskA hybrid sensor kinase controls the composition of the electron transport chain. *Environ Microbiol Rep* **5**: 291-300.

Shingler, V. (2003) Integrated regulation in response to aromatic compounds: from signal sensing to attractive behaviour. *Environ Microbiol* **5**: 1226-1241.

Sonnleitner, E., Hagens, S., Rosenau, F., Wilhelm, S., Habel, A., Jager, K.E., and Bläsi, U. (2003) Reduced virulence of a *hfq* mutant of *Pseudomonas aeruginosa* O1. *Microb Pathog* **35**: 217-228.

Sonnleitner, E., Schuster, M., Sorger-Domenigg, T., Greenberg, E.P., and Bläsi, U. (2006) Hfq-dependent alterations of the transcriptome profile and effects on quorum sensing in *Pseudomonas aeruginosa*. *Mol Microbiol* **59**: 1542-1558.

Sonnleitner, E., Abdou, L., and Haas, D. (2009) Small RNA as global regulator of carbon catabolite repression in *Pseudomonas aeruginosa*. *Proc Natl Acad Sci USA* **106**: 21866-21871.

Sonnleitner, E., and Bläsi, U. (2014) Regulation of Hfq by the RNA CrcZ in *Pseudomonas aeruginosa* carbon catabolite repression. *PLoS Genet* **10**: e1004440.

Sonnleitner, E., Wulf, A., Campagne, S., Pei, X.Y., Wolfinger, M.T., Forlani, G. et al. (2017) Interplay between the catabolite repression control protein Crc, Hfq and RNA in Hfq-dependent

translational regulation in *Pseudomonas aeruginosa*. *Nucleic Acids Res* **gkx1245,** https://doi.org/10.1093/nar/gkx1245.

Swingle, B., Thete, D., Moll, M., Myers, C.R., Schneider, D.J., and Cartinhour, S. (2008) Characterization of the PvdS-regulated promoter motif in *Pseudomonas syringae* pv. *tomato* DC3000 reveals regulon members and insights regarding PvdS function in other pseudomonads. *Mol Microbiol* **68**: 871-889.

Tiburzi, F., Imperi, F., and Visca, P. (2008) Intracellular levels and activity of PvdS, the major iron starvation sigma factor of *Pseudomonas aeruginosa*. *Mol Microbiol* **67**: 213-227.

Udaondo, Z., Molina, L., Segura, A., Duque, E., and Ramos, J.L. (2016) Analysis of the core genome and pangenome of *Pseudomonas putida*. *Environ Microbiol* **18**: 3268-3283.

Ugidos, A., Morales, G., Rial, E., Williams, H.D., and Rojo, F. (2008) The coordinate regulation of multiple terminal oxidases by the *Pseudomonas putida* ANR global regulator. *Environ Microbiol* **10**: 1690–1702.

Updegrove, T.B., Zhang, A., and Storz, G. (2016) Hfq: the flexible RNA matchmaker. *Curr Opin Microbiol* **30**: 133-138.

Valentini, M., and Lapouge, K. (2013) Catabolite repression in *Pseudomonas aeruginosa* PAO1 regulates the uptake of C4-dicarboxylates depending on succinate concentration. *Environ Microbiol* **15**: 1707-1716.

Valentini, M., García-Mauriño, S.M., Pérez-Martínez, I., Santero, E., Canosa, I., and Lapouge, K. (2014) Hierarchical management of carbon sources is regulated similarly by the CbrA/B systems in *Pseudomonas aeruginosa* and *Pseudomonas putida*. *Microbiology* **160**: 2243-2252.

Visca, P., Leoni, L., Wilson, M.J., and Lamont, I.L. (2002) Iron transport and regulation, cell signalling and genomics: lessons from *Escherichia coli* and *Pseudomonas*. *Mol Microbiol* **45**: 1177-1190.

Vogel, J., and Luisi, B.F. (2011) Hfq and its constellation of RNA. *Nat Rev Microbiol* **9**: 578-589.

Wagner, E.G., and Romby, P. (2015) Small RNAs in Bacteria and Archaea: Who They Are, What They Do, and How They Do It. *Adv Genet* **90**: 133-208.

Watson, R.J., Millichap, P., Joyce, S.A., Reynolds, S., and Clarke, D.J. (2010) The role of iron uptake in pathogenicity and symbiosis in *Photorhabdus luminescens* TT01. *BMC Microbiol* **10**: 177.

Wessel, D., and Flugge, U.I. (1984) A method for the quantitative recovery of protein in dilute solution in the presence of detergents and lipids. *Anal Biochem* **138**: 141-143.

Wilderman, P.J., Sowa, N.A., FitzGerald, D.J., FitzGerald, P.C., Gottesman, S., Ochsner, U.A., and Vasil, M.L. (2004) Identification of tandem duplicate regulatory small RNAs in *Pseudomonas aeruginosa* involved in iron homeostasis. *Proc Natl Acad Sci USA* **101**: 9792-9797.

Woodcock, D.M., Crowther, P.J., Doherty, J., Jefferson, S., DeCruz, E., Noyer-Weidner, M. et al. (1989) Quantitative evaluation of *Escherichia coli* host strains for tolerance to cytosine methylation in plasmid and phage recombinants. *Nucleic Acids Res* **17**: 3469-3478.

Wu, X., Monchy, S., Taghavi, S., Zhu, W., Ramos, J., and van der Lelie, D. (2011) Comparative genomics and functional analysis of niche-specific adaptation in *Pseudomonas putida*. *FEMS Microbiol Rev* **35**: 299-323.

Yuste, L., Canosa, I., and Rojo, F. (1998) Carbon-source-dependent expression of the *PalkB* promoter from the *Pseudomonas oleovorans* alkane degradation pathway. *J Bacteriol* **180**: 5218-5226.

Yuste, L., Hervás, A.B., Canosa, I., Tobes, R., Jiménez, J.I., Nogales, J. et al. (2006) Growth-phase dependent expression of the *Pseudomonas putida* KT2440 transcriptional machinery analyzed with a genome-wide DNA microarray. *Environ Microbiol* **8**: 165-177.

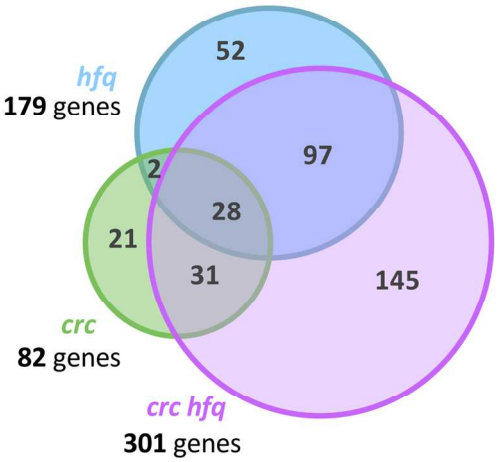

Most relevant genes/functions altered in:

-Hfq-null strain
- Prophages
- Iron metabolism
- Electron transport chain
- Carbon metabolism
- Porins

-Crc-null strain
- Iron metabolism
- Sulphur metabolism
- Cytochromes

-Crc/Hfq-null strain
- Those of the Hfq-null strain plus:
- Intermediary metabolism
- Chemotaxis

Figure 1

77x43mm (600 x 600 DPI)

A

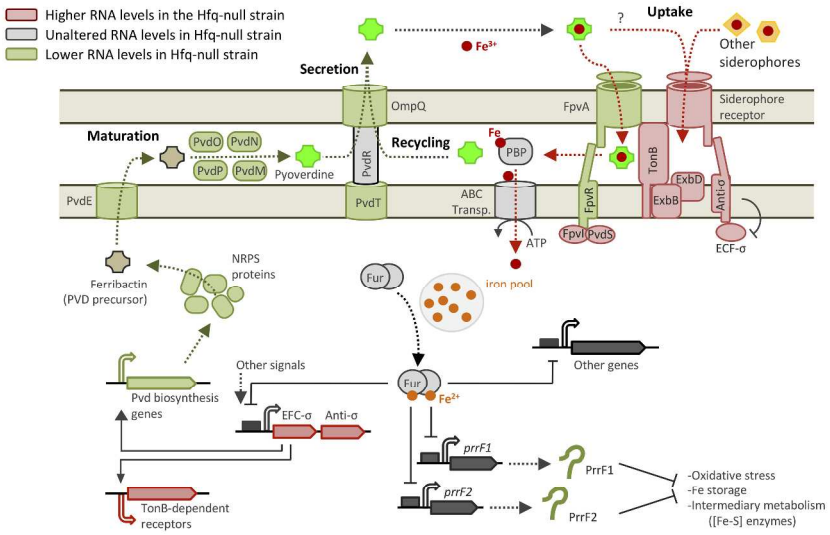

B

Downregulated iron-uptake genes		Upregulated iron-uptake genes		Iron / heme uptake	
PP_0272[1]	Ferric siderophore receptor	PP_0160[3]	TonB-dep. siderophore recept., *foxA*	PP_4687[2,3]	Hemin import ATP-binding prot. *hmuV*
PP_2901[1,2]	Acyl-homoserine lactone acylase, *pvdQ*	PP_0161[2,3]	Transmemb. anti-sigma factor, *foxR*		
PP_3555[2]	Anti-sigma factor, *fpvR*	PP_0267[2,3]	Ferric siderophore receptor	PP_4688[2,3]	Heme/hemin ABC trnsp. perm. *phuU*
PP_3796[1,2,3]	L-ornithine N5-oxygenase, *pvdA*	PP_0351[2,3]	Transmemb. anti-sigma factor, *fiuR*		
PP_3797[3]	Probable pyoverdine biosynth. prot., *fpvG*	PP_0352[3]	ECF-7 sigma factor, *fiuI*	PP_4264[2,3]	Oxygen-indp. copro-porphyrinogen III oxidase, *hemN*
PP_3798[2,3]	Probable pyoverdine biosynth. prot., *fpvH*	PP_0668[2,3]	Transmembrane sensor		
PP_3799[2,3]	Probable pyoverdine biosynth. prot., *fpvJ*	PP_0667[3]	ECF-15 sigma factor		
PP_3800[2,3]	Probable pyoverdine biosynth. prot., *fpvK*	PP_0700[3]	Transmembrane anti-sigma factor		
PP_3801[2,3]	Cation ABC transporter, probable *fpvC*	PP_0703[3]	Transmembrane anti-sigma factor		
PP_3802[2,3]	Cation ABC transporter, probable *fpvD*	PP_0704[3]	ECF-16 sigma factor		
PP_3803[2,3]	Cation ABC transporter, probable *fpvE*	PP_0861[2,3]	Ferric siderophore receptor		
PP_3804[2,3]	Metal ion transport, problable *fpvF*	PP_2192[3]	Hybrid ECF/anti-sigma factor, *iutY*		
PP_4210[1]	Pyoverdine ABC transporter, *pvdT*	PP_2193[3]	Aerobactin receptor, *iutA*		
PP_4211[1,3]	Pyoverdine efflux protein, *ompQ*	PP_3084[2,3]	Ferric siderophore receptor		
PP_4212[1,3]	Pyoverdine biosynthesis protein, *pvdP*	PP_3085[3]	Transmembrane anti-sigma factor		
PP_4213[3]	Dipeptidase, *pvdM*	PP_3086[3]	ECF-9 sigma factor		
PP_4214[1,3]	Pyoverdine biosynthesis protein, *pvdN*	PP_3155[2,3]	Ferric siderophore receptor		
PP_4215[1,2,3]	Pyoverdine biosynthesis protein, *pvdO*	PP_3612[2,3]	TonB-dependent receptor		
PP_4216[1,2,3]	Pyoverdine ABC export system, *pvdE*	PP_4208[2,3]	ECF-6 sigma factor, *fpvI*		
PP_4217[2,3]	Ferripyoverdine receptor, *fpvA*	PP_4244[2,3]	ECF-4 sigma factor, *pvdS*		
PP_4218[1,2,3]	Lipase/esterase family protein	PP_4607[2,3]	Transmembrane anti-sigma factor		
PP_4219[1,2,3]	Non-ribosomal peptide synthetase, *pvdD*	PP_4608[2,3]	ECF-5 sigma factor		
PP_4220[1,2,3]	Non-ribosomal peptide synthetase, *pvdJ*	PP_4611[3]	ECF-2 sigma factor, *fecI*		
PP_4221[1,2,3]	Non-ribosomal peptide synthetase, *pvdI*	PP_4612[3]	FecR anti-sigma factor		
PP_4222[1,2,3]	Non-ribosomal peptide synthesis, *syrP*	PP_5196[2,3]	Iron ABC trnp. subst. bind. prot. *fbpA*		
PP_4223[1,2,3]	Diaminobutyrate-2-oxoglut. transam., *pvdH*	PP_5308[2,3]	Ferric sideroph. transp. *tonB*		
PP_4243[1,2,3]	Non-ribosomal peptide synthetase, *pvdL*	PP_5307[1,2,3]	Ferric sideroph. transp. *exbD*		
PP_4245[1,2,3]	Hydroxyproline acetylase, *pvdY*	PP_5306[2,3]	Ferric sideroph. transp. *exbB*		

Iron storage	
PP_0482[2,3]	Bacterioferritin, *bfrα*
PP_1082[2,3]	Bacterioferritin, *bfrβ*
PP_1083[3]	Bacterioferritin-associated ferredoxin

Red: Higher RNA levels than in wt
Green: Lower RNA levels than in wt
(1) In Crc-null strain
(2) In Hfq-null strain
(3) In Crc/Hfq-null strain

Figure 2

207x252mm (600 x 600 DPI)

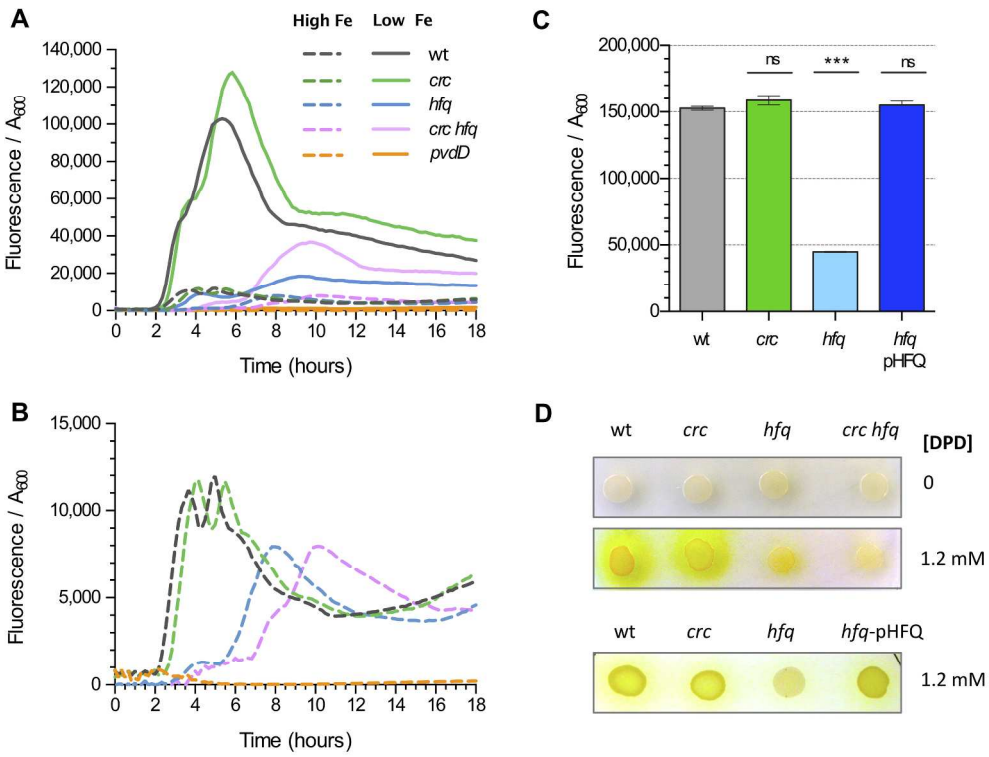

Figure 3

121x91mm (600 x 600 DPI)

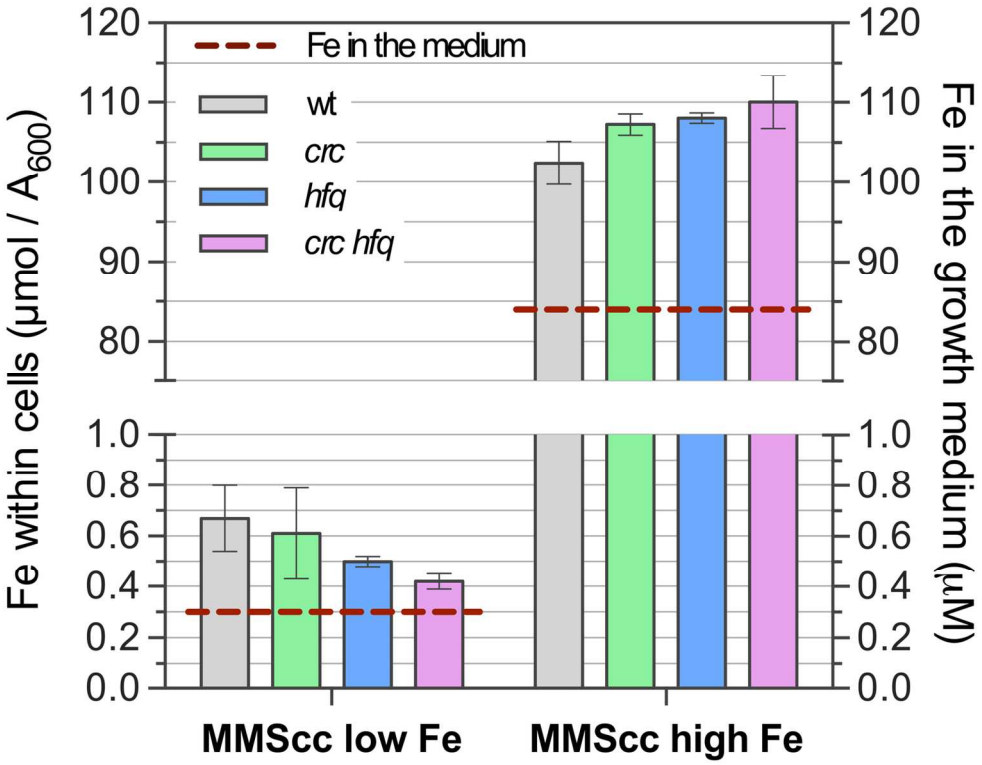

Figure 4

69x54mm (600 x 600 DPI)

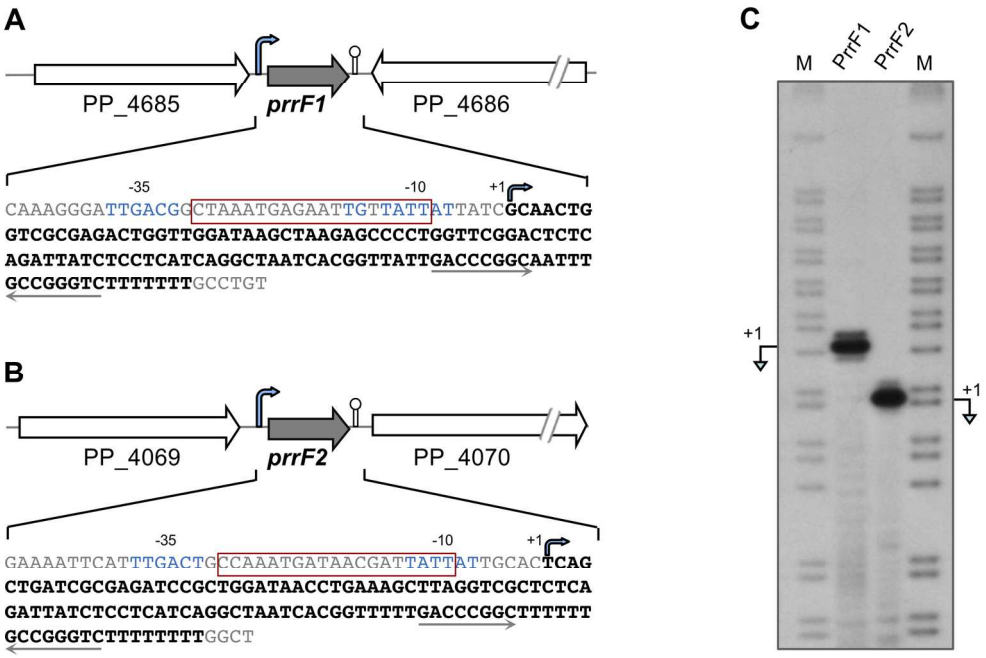

Figure 5

86x58mm (600 x 600 DPI)

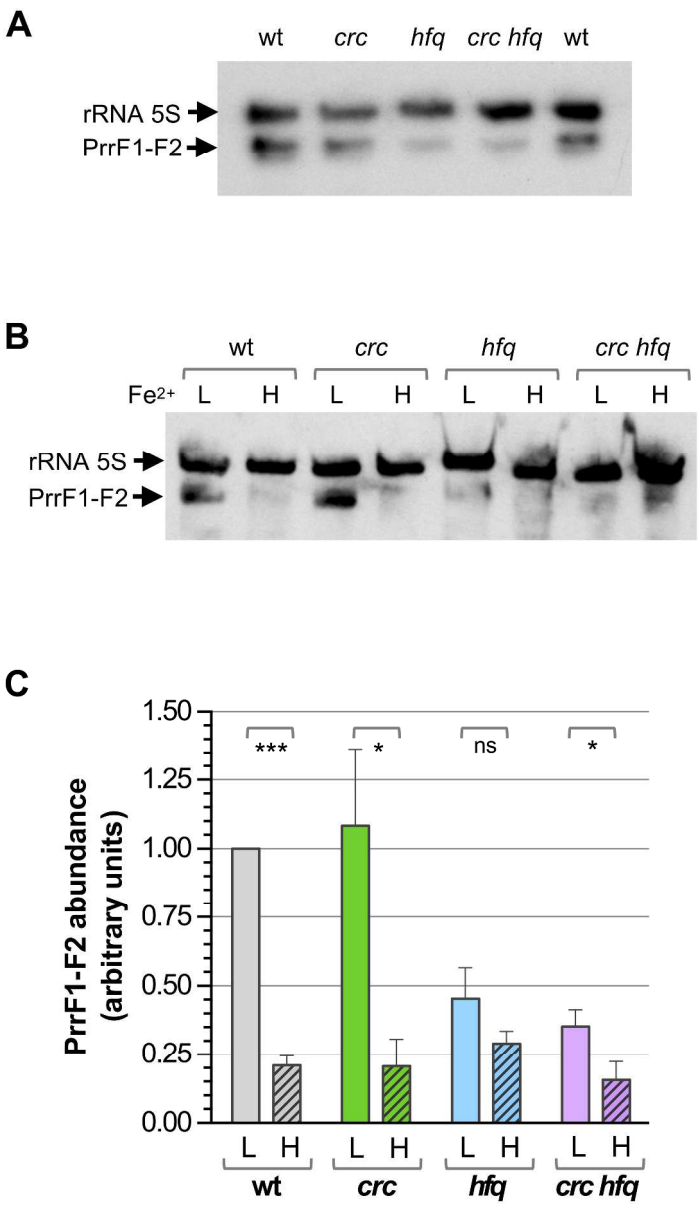

Figure 6

125x212mm (600 x 600 DPI)

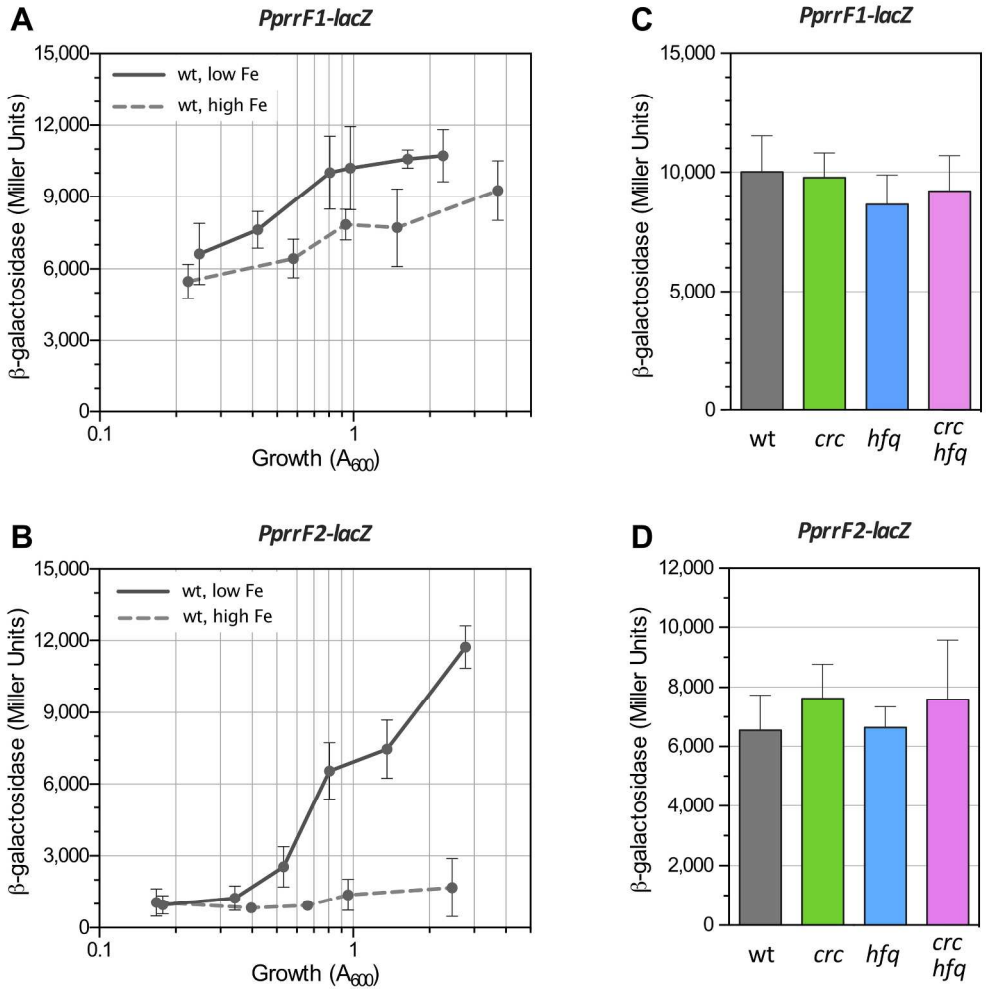

Figure 7

118x118mm (600 x 600 DPI)